

1 **Cellulose-deconstruction potential of nano-biocatalytic systems: A strategic drive**
2 **from designing to sustainable applications of immobilized cellulases**

3 Sarmad Ahmad Qamar¹, Mahpara Qamar¹, Muhammad Bilal^{2,*}, Ram Naresh

4 Bharagava³, Luiz Fernando Romanholo Ferreira^{4,5}, Farooq Sher⁶, Hafiz M.N. Iqbal^{7,*}

5 ¹Department of Biochemistry, University of Agriculture, Faisalabad, Pakistan.

6 ²School of Life Science and Food Engineering, Huaiyin Institute of Technology, Huaian,
7 223003, China.

8 ³Laboratory of Bioremediation and Metagenomics Research (LBMR), Department of
9 Microbiology (DM), Babasaheb Bhimrao Ambedkar University (A Central University),
10 Vidya Vihar, Raebareli Road, Lucknow 226 025 U.P., India.

11 ⁴Waste and Effluent Treatment Laboratory, Institute of Technology and Research (ITP),
12 Tiradentes University, Farolândia, Aracaju-SE, 49032-490, Brazil.

13 ⁵Graduate Program in Process Engineering, Tiradentes University (UNIT), Av. Murilo
14 Dantas, 300, Farolândia, 49032-490, Aracaju-Sergipe, Brazil.

15 ⁶Department of Engineering, School of Science and Technology, Nottingham Trent
16 University, Nottingham NG11 8NS, UK.

17 ⁷Tecnologico de Monterrey, School of Engineering and Sciences, Monterrey, 64849,
18 Mexico.

19 *Corresponding authors emails: bilaluaf@hotmail.com (M. Bilal); hafiz.iqbal@tec.mx
20 (H.M.N. Iqbal).

21
22 **Abstract**

23 Nanostructured materials along with an added value of polymers-based support carriers
24 have gained high interest and considered ideal for enzyme immobilization. The recently
25 emerged nanoscience interface in the form of nanostructured materials combined with
26 immobilized-enzyme-based bio-catalysis has now become research and development
27 frontiers in advance and applied bio-catalysis engineering. With the involvement of
28 nanoscience, various polymers have been thoroughly developed and exploited to
29 nanostructured engineer constructs as ideal support carriers/matrices. Such
30 nanotechnologically engineered support carriers/matrix possess unique structural,
31 physicochemical, and functional attributes which equilibrate principal factors and

32 strengthen the biocatalysts efficacy for multipurpose applications. In addition, nano-
33 supported catalysts are potential alternatives that can outstrip several limitations of
34 conventional biocatalysts, such as reduced catalytic efficacy and turnover, low mass
35 transfer efficiency, instability during the reaction, and most importantly, partial, or
36 complete inhibition/deactivation. In this context, engineering robust and highly efficient
37 biocatalysts is an industrially relevant prerequisite. This review comprehensively covered
38 various biopolymers and nanostructured materials, including silica, hybrid nanoflower,
39 nanotubes or nanofibers, nanomembranes, graphene oxide nanoparticles, metal-oxide
40 frameworks, and magnetic nanoparticles as robust matrices for cellulase immobilization.
41 The work is further enriched by spotlighting applied and industrially relevant
42 considerations of nano-immobilized cellulases. For instance, owing to the cellulose-
43 deconstruction features of nano-immobilized cellulases, the applications like
44 lignocellulosic biomass conversion into industrially useful products or biofuels, improved
45 paper sheet density and pulp beat in paper and pulp industry, fruit juice clarification in
46 food industry are evident examples of cellulases, thereof are discussed in this work.

47 **Keywords:** Cellulose-deconstructing enzymes; Immobilization; Nanostructured carriers;
48 Polymeric supports; Bio-catalysis; Sustainability; Food industry

49

50 **1. Introduction**

51 Enzymes are extremely efficient biocatalysts being extensively employed in various
52 industrial and biotechnological processes. Cellulase (EC 3.2.1.4) is one of the important
53 enzymes, frequently used for the hydrolysis of 1,4-glycosidic linkages among cellulose
54 molecules to synthesize monosaccharides subunits. Cellulases exhibit numerous
55 applications in pharmaceutical, pulp & paper, detergents, chemical, food, and biomedical
56 sectors [1-4]. Moreover, cellulases could be employed for the fermentation of
57 lignocellulosic biomass to produce biofuels [5-8]. However, much concern has been
58 devoted towards the stability and reusability of cellulases that restricted its industrial
59 applications [9-13]. Recently, the microbial production of cellulases using cost-effective
60 methodologies, and to overcome the research challenges has been remarkably
61 considered for the cellulases to improve industrial applications [14,15]. Although cellulase
62 enzyme exhibit several applications in industrial and biomedical sectors, majority of these

63 cellulase types suffer from low pH and thermal stabilities in various media. Moreover, their
64 utilization is also restricted because of their lack of recyclability. Various methods e.g.,
65 chemical modifications, protein engineering, and their immobilization in different
66 biopolymers and nanomaterials could be used to enhance enzymatic stability and
67 recyclability potential [10,11,13,14,16]. Figure 1 shows significant potential of
68 nanomaterials for enzyme immobilization [17]. Among all, immobilization provides more
69 benefits regarding heterogeneous catalytic reactions and to overcome the lack of
70 recyclability [18,19].

71 Immobilization methodologies could be divided into three major classes such as (i)
72 surface immobilization [20,21]; (ii) self-immobilization [22]; and (iii) entrapment [23-25].
73 These methodologies are extensively adopted for the immobilization of biocatalysts that
74 could be inorganic or organic, e.g., polymers, polysaccharides, proteins, activated carbon,
75 and metal nanoparticles [13,16,26]. However, the efficiency of immobilized biocatalyst on
76 its stability, support separation from product, extent of recyclability, and the activity after
77 immobilization are the key factors which are carefully considered while using a support
78 material [10]. Among all supports, nanostructured materials have special place regarding
79 their distinguished high surface area along with other characteristic features that enable
80 higher enzyme loading efficacy (Figure 2) [17,22,27]. However, the enzymes
81 immobilization using nanostructured materials may be restricted due to the issues with
82 recovery, such as filtration or centrifugation for industrial biotechnological applications,
83 which have created serious issues with the processes e.g., extraction and purification of
84 enzymes. These limitations could be removed by employing magnetic nanoparticles as a
85 promising support material for biomolecules e.g., nucleic acids, antibodies, enzymes, and
86 peptides, with high recovery and recyclability potential [9,28]. The convenient process for
87 the recovery of magnetic nanocarriers from the reaction mixture could be the employment
88 of magnetic field and their less toxic nature make these nano-supports as promising
89 materials for enzyme immobilization [9,22,29]. Except these several biopolymer and
90 nano-structured supports have also been employed for the immobilization of cellulases
91 for functional applications.

92 Typically, there are four different immobilization modes of enzymes e.g., entrapment,
93 covalent attachment, physical adsorption, and crosslinking. Attachment of enzymes and

94 support matrix can be covalently or weakly and physical or chemical [10]. Physical
95 attachment of enzyme with support matrix is relatively weaker than covalent binding, and
96 it has lower capability of keeping enzyme fixed to the support matrix. The support
97 materials are generally polymers/biopolymers, and nanocarriers. In entrapment, the
98 enzymes are integrated on a membrane apparatus such as polymer network e.g., an
99 organic polymer or a silica sol-gel, desolate fiber, or a microcapsule. The formation of a
100 polymer network is required for entrapment in the presence of enzyme. The formation of
101 enzyme aggregates or crosslinking crystals by the utilization of crosslinking or bifunctional
102 agent is another mode of immobilization of enzymes [30]. Carrier-binding or physical
103 adsorption mode of immobilization uses water-insoluble carriers e.g., synthetic polymers,
104 polysaccharide derivatives, and glass [31,32]. In covalent binding or crosslinking,
105 crosslinker reagent e.g., hexamethylene diisocyanate, bisdiazobenzidine, and
106 glutaraldehyde are required [33]. Different polymers such as carrageenan, collagen, and
107 cellulose are used by entrapment mode. However, membrane confinement require the
108 formation of microcapsules and liposomes [34,35].

109 Immobilization of enzymes using membrane entrapment method is reported to be an
110 excellent biochemical engineering approach because it enable continuous operations,
111 stability enhancement, and retention in bioreactors. In membrane bioreactor, physical
112 adsorption immobilization reduce the loss of catalytic activity of enzymes and enhance
113 the recyclability potential ultimately decreasing the bioprocess cost [36]. The enzyme
114 immobilization is preferred over free enzymes due to its long-term availability that reduce
115 the excessive purification methodologies. The enzyme recovery method could be the
116 ultrafiltration which require the utilization of membrane systems allowing the passage of
117 small molecules and keeping the enzyme in bioreactors. Membrane fouling is another
118 important factor to consider while the operation and development of membrane system
119 because it effects the performance, operational cost, cleaning needs, and pretreatment
120 requirements [37]. There are few other modes of enzymatic immobilization which could
121 be the combination of above-mentioned processes, which are particular for specific
122 enzyme or matrix. Nevertheless, not a single method or support matrix is efficient for all
123 enzyme kinds and their usage because of array of different product utilization,
124 characteristics of enzymes, substrates, and products, and the chemical composition.

125 This review discusses the current advancements in engineering aspects of novel nano-
126 structured and biopolymer-based support materials for their effective deployment for
127 cellulase immobilization (Figure 3). Moreover, the exceptional features of various
128 nanomaterials such as silica, hybrid nanoflower, carbon nanotubes/nanofibers,
129 nanomembranes, graphene oxide nanoparticles, and metal-oxide frameworks have also
130 been reviewed as robust matrices for cellulase immobilization. Several biotechnological
131 applications of immobilized cellulases such as cellulose hydrolysis, pulp and paper
132 industry, food industry, and other potential multifunctional applications have also been
133 reviewed in this article.

134 **2. Immobilization of cellulases on polymers-based supports**

135 **2.1 Cellulases immobilization on Ca-alginate**

136 Ca-alginate entrapment is an important strategy for the immobilization of enzymes [25].
137 Alginates are biopolymers which are commonly present in the market as water soluble
138 Na-alginates. Ca-alginate entrapment is recognized as inexpensive, non-toxic, rapid, and
139 versatile technique for the immobilization of various cells and enzymes [38]. Alginates are
140 biopolymers obtained from marine plants, composed of unbranched linear polymer chains
141 consisting of α -(1,4)-linked L-guluronic acid, and β -(1,4)-linked D-mannuronic acid
142 residues. It results in the development of thermostable and biocompatible hydrogels in
143 the occurrence of Ca^{2+} ions [39,40]. The use of alginate as immobilization support for
144 bioprocessing application provides high thermo- and pH stable gels to use at room
145 temperature. Alginates synthesize gels with most divalent and multivalent cations. In
146 addition, the gelation could not be induced by Mg^{2+} and monovalent ions, however, Sr^{2+}
147 and Ba^{2+} induce stronger alginate gels than Ca^{2+} . However, the use of Ca-alginate gels
148 for enzymes immobilization has commonly been reported [25,41-43].

149 Andriani et al. [41] studied the immobilization of cellulase produced by *Bacillus subtilis*
150 strain isolated from puffer fish, using carboxy methyl cellulase (CMC) as substrate and
151 Ca-alginate as support-material. Different factors were optimized such as calcium
152 chloride concentration, sodium alginate concentration, pH, and temperature. The enzyme
153 showed high stability at pH 6, however, no changes were observed at maximum pH
154 before and after immobilization. The enzyme with greater stability was achievable at the
155 2% sodium alginate and 0.15 M calcium chloride solution. As compared to the free

156 enzyme, the slight increase in K_m and V_{max} was attained by kinetic studies. The
157 immobilized enzyme showed high recyclability up to four times without significant loss in
158 initial activity. The enzyme lost its activity at 30 °C within three days but the storage
159 stability was more efficient at 4 °C and remained active up to 12 days [41]. Similarly, Viet
160 et al. [44] studied cellulase immobilization using Ca-alginate entrapment. The 2% of
161 sodium alginate content was reported efficient for the formation of stable alginate beads.
162 The CMC was used as a substrate to analyze the cellulase activity. The beads with 3 mm
163 diameter and 30 min immobilized time showed the maximum (83.645%) efficiency for
164 enzyme immobilization. The optimum pH 4.5 was observed for cellulase immobilization.
165 As compared to the free cellulase, the highest optimum temperature of 55 °C and 60 °C
166 was calculated from immobilized enzyme. The 69.2% activity retention after 5 consecutive
167 cycles indicated good storage stability of immobilized enzyme [44].

168 Sankarraj and Nallathambi, [45] immobilized cellulase enzyme on to hybrid Con-A
169 (concanavalin A) covered by the calcium alginate–starch beads. The jack beans were
170 used to isolate the Con-A and SDS-PAGE analysis was used for the determination of
171 crude protein. The high storage stability and mechanical properties were observed by the
172 immobilized cellulase that even after a month of incubation, showed 100% and 85%
173 activities at 4 °C and 30 °C, respectively. The free form of enzyme maintained 20% of its
174 activity even after 5 consecutively repeated experiments, however, the immobilized
175 cellulase retained 70% of its activity that demonstrates its better thermal stability after
176 immobilization. The research provided a facile process for the immobilization of cellulase
177 for improved stability and recyclability perspective [45]. Another study conducted by
178 Abdel-Sater et al. [46] reported cellulase production by *Penicillium brevicompactum*
179 specie and the enzyme was immobilized in Chitosan-alginate beads using magnetic
180 nanocarriers and glutaraldehyde as crosslinking agents. The optimizational results
181 indicated pH 6 and 30 °C temperature to achieve the maximum cellulase activity in the
182 medium containing sodium nitrate and palm date leaves incubated for 9 days. The high
183 structural stability was observed after the ammonium sulfate precipitation due to the two-
184 folded increase in enzymatic activities. It was observed that acidic pH and high
185 temperature favors the precipitated enzyme. The maximum activity at pH 5.5 and 50 °C
186 temperature was achieved by immobilized cellulase which was remained excellent up to

187 80 °C. Different conditions such as resistant to microbial invade, nontoxicity,
188 biocompatibility, easy synthesis, and moderate gelatin conditions play important role for
189 the desirability of enzyme encapsulated within alginate beads. For different
190 biotechnological and industrial demands, the immobilized enzyme shows the usefulness
191 proven by the study [46].

192 In a recent report, Imran et al. [42] studied the production of cellulase from *Aspergillus*
193 *tubingensis*, and the enzyme was immobilized using Ca-alginate as support material. The
194 excellent increase in catalytic activity and stability was determined. As compared to the
195 free enzyme after 26 h incubation, the immobilized cellulase showed 82% thermostability
196 at high temperature (75 °C). For both free and Ca-alginate immobilized cellulase, the
197 enzymatic activities were decreased after the 20th day of incubation. The activity of
198 cellulase ($179 \pm 0.4 \text{ U mL}^{-1} \text{ min}^{-1}$) for xerogel matrix was obtained at 45 °C and it exhibited
199 the activity of ($174 \pm 0.4 \text{ U mL}^{-1} \text{ min}^{-1}$) at pH 4.5. The highest K_m values were noticed for
200 the immobilized enzyme as compared to the free cellulase; however, lowest K_m was
201 observed by xerogel immobilized enzyme. The enhanced tolerance capacity of 75–82%
202 was observed for the immobilized cellulase on Ca-alginate and xerogel matrix in
203 opposition of activators and or inhibitors like EDTA, SDS, Hg^{2+} , Co^{2+} , and Ca^{2+} [42]. These
204 studies proved the immobilized cellulase as an excellent candidate for industrial and
205 biotechnological uses due to enhanced fruit juice saccharification.

206 **2.2 Cellulases immobilization on chitosan**

207 Chitosan as a functional material, offers various desirable characteristics including
208 hydrophilicity, gel forming properties, heavy metal ions chelation, antibacterial properties,
209 physiological inertness, nontoxicity, biodegradability, biocompatibility, and remarkable
210 affinity to proteins. Due to these novel features, chitosan-based materials are yet under-
211 studied, and can be expected to be frequently explored in near future for various
212 bioprocessing applications including immobilization supports [25,47,48]. For instance,
213 Abd El-Ghaffar and Hashem, [49] studied the immobilization of cellulase enzyme onto
214 chitosan, chitosan–4-amino butyric acid, and chitosan–L-glutamic acid supports using
215 covalent crosslinking approach. The assay was performed at 25 °C and pH 7, and
216 retention in cellulase activities were observed for the chitosan, chitosan–4-aminobutyric
217 acid crosslinked with 1% of glutaric dialdehyde, and chitosan–L-glutamic acid as 65.52%,

218 63.19%, and 85.32%. As compared with free enzyme, immobilized enzyme exhibited
219 better pH, thermal, and storage stability profiles. The immobilized enzyme maintained
220 60% of its initial activity 6-times from its original activity after the immobilization on
221 chitosan-GDA (1%). The change was not observed even after the 10th cycle for chitosan-
222 glutamic acid-GDA (1%) and chitosan-4-aminobutyric acid–GDA (1%) immobilized
223 cellulase. For above-mentioned carriers, the 70% and 50% of activities were maintained
224 after the 25 consecutively repeated experiments [49]. Similarly, Miao et al. [50] used
225 Fe₃O₄ nanoparticles onto chitosan for direct immobilization of cellulases *via*
226 glutaraldehyde crosslinking to form nano-supports of magnetic chitosan microspheres.
227 Different conditions for enzyme immobilization were also optimized which indicated 5 h
228 incubation, 15 mL (0.1 mg/mL) enzyme, temperature 30 °C and pH 7. The enzymatic
229 recovery was 73.5 mg/g (71.6%) of maximum solid loading rate was observed for
230 medium-chain triglycerides (MCTs) at optimized conditions. The immobilized cellulase
231 can be regenerated and reused without significant loss in activity for 3 consecutive
232 experiments. However, the better storage stability and thermal optima were observed for
233 the immobilized cellulase as compared with free cellulase [50].

234 Sánchez-Ramírez et al. [28] studied the production and immobilization of *Trichoderma*
235 *reesei* cellulase using chitosan-coated magnetic nanocarriers as support material *via*
236 glutaraldehyde as coupling agent. Magnetic nanocarriers (around 10 nm diameter) were
237 formed after cellulase immobilization however, 8 nm diameter was observed before
238 immobilization. The enhanced thermal and storage stability was analyzed for immobilized
239 cellulase along with the 37% retention of initial activity. The magnetic field was applied to
240 separate the cellulase and after 15 cycles of CMC hydrolysis, immobilized enzyme
241 maintained around 80% of its initial activity. Kinetic studies indicated about 8 times
242 increase in K_m value of immobilized enzymes as compared with free enzyme. The
243 hydrolyzed *Agave atrovirens* leaves-based lignocellulosic material showed the ability to
244 reuse in material hydrolysis up to four consecutively repeated experiments with 50 % of
245 activity retention. Lignocellulose hydrolysis showed the yield near to the activity obtained
246 from free enzyme [28]. Similarly, Díaz-Hernández et al. [51] studied cellulase and
247 xylanase immobilization by chitosan coated magnetic iron oxide nanoparticles produced
248 in single step *via* alkaline precipitation to get maximum enzyme loading. Overall, 93%

249 magnetic saturation of the magnetite was achieved by the crosslinking of chitosan-coated
250 magnetite particles (Fe_3O_4 @chitosan) with cellulase and xylanase enzymes. The
251 characterizational analysis indicated that the 12 mg enzyme per 1 g of magnetic support,
252 and 162 mg of chitosan was coated on 1 g of nanocomposite. The crosslinking between
253 cellulase and Fe_3O_4 @chitosan support was confirmed by characterization analysis. The
254 average particle size of 230–430 nm was reported for supports before and after
255 immobilization [51].

256 Mo et al. [52] used sugarcane bagasse to prepare the porous biochar which was covered
257 with varying quantities of chitosan for cellulase immobilization using glutaraldehyde as
258 the crosslinker (Figure 4). Characterizational analysis indicated that high thermal and pH
259 stability after immobilization. Furthermore, the good reusability and activity was also
260 observed for these three types of immobilized cellulases. For cellulase@CS25, the
261 support maintained the better morphology of porous biochar with the feeding ratio
262 (biochar: chitosan, 0.5 g:25 mg). The associated immobilized cellulase demonstrated the
263 90.8 % of glucose production even after 10 repeated experiments and maintained 67 %
264 activity of free enzyme at pH 4 and 60 °C [52]. In another study, Mo and Qiu, [53] prepared
265 porous biochar by pyrolyzing sugarcane bagasse followed by calcination for the
266 magnetization with $\gamma\text{-Fe}_2\text{O}_3$. The synthesized chitosan/magnetic porous biochar was
267 employed as an immobilization support material for cellulase by covalent bonding after
268 fabrication with chitosan activated by glutaraldehyde. The pH 5 and temperature 25 °C
269 for 12 h of incubation showed 80.5 mg cellulase/g support amount for efficient
270 immobilization of cellulase. Varying pH and temperature were used to study the CMC
271 hydrolysis Both free and immobilized enzymes showed optimum values as pH 4 and
272 temperature of 60 °C. The relatively high enzyme recovery of 73.0% was recorded for the
273 immobilized cellulase. Moreover, the slower maximum reaction velocity (V_{max}) and higher
274 K_m values were reported than free cellulase [53].

275 **2.3 Cellulases immobilization on hybrid polymers-based supports**

276 Various hybrid polymer-based support matrices have been reported for the immobilization
277 of cellulases for bioprocessing applications. For instance, the use of reversible insoluble-
278 soluble enteric polymer coupled with carbodiimide to perform covalent immobilization of
279 a commercial cellulase was performed by Yu et al. [54]. The binding efficiency (81.08%)

280 of covalently immobilized Eudragit-cellulase was greater as compared with non-covalent
281 Eudragit-cellulase (56.83%). The optimum pH 5 and temperature 50 °C caused the
282 increase in the relative activity of both immobilized and free cellulase; however, more
283 increase in pH and temperature showed the negative impacts on the activity of both native
284 cellulase and covalent Eudragit-cellulase. The higher pH and temperature showed higher
285 stability for the covalent Eudragit-cellulase. The free cellulase had the K_m value of 2.89
286 g/L, less than that of covalent Eudragit-cellulase (4.78 g/L). The immobilization on the
287 Eudragit S-100 tend to increase the affinity of the cellulase to its substrate [54].

288 Ince et al. [55] used surface initiated-atomic transfer radical polymerization for grafting
289 the poly(styrene-divinylbenzene) (PS-DVB) microspheres with the polystyrene. In next
290 step, sulfuric acid in the existence of P_2O_5 was used to proceed the sulfonation of the
291 grafted polystyrene chains. Aniline (4.8 mmol/g) was applied on the surface to neutralize
292 the sulfonic acid groups. The oxidation of potassium persulfate was carried out to provide
293 the self-doped and thick (16 μm) PANI layers on the microstructures. The oxidized
294 potassium persulfate was further used to polymerize the adsorbed aniline achieved by
295 previous stage. The adsorption/crosslinking methodologies were used to immobilize the
296 cellulase on the polyaniline coated PS-DVB-*g*-PS micro-spheres. As compared with free
297 enzyme, the immobilized cellulase had the excellent storage stability, higher maintenance
298 of activities relative to the temperature and pH [55]. Similarly, Romo-Sánchez et al. [56]
299 studied immobilization of two enzymes (cellulase and xylanase) on two polymeric support
300 matrices (alginate-chitin and chitosan-chitin) *via* different chemical ways such as
301 crosslinking-adsorption, reticulation, and adsorption to improve stability and recyclability
302 of enzymes. The chitosan polymer was proved as an ideal support by giving 170 $\mu\text{g/mL}$
303 of optimal enzyme concentration for cellulase. However, 127.5 $\mu\text{g/mL}$ for the xylanase.
304 Moreover, the optimal pH binding of cellulase was 4.5 and for xylanase was 5.0. The
305 immobilization procedure showed the better stability after the application of lower
306 amounts of glutaraldehyde. The use of glutaraldehyde enabled the activity retention up
307 to 64% after immobilization of cellulase for 19 cycles [56].

308 The use of core-shell polymer-protein nanocarriers for cellulase immobilization was
309 reported by a recent study [57]. The immobilization of His6-tagged cellulases with
310 controlled spatial orientation of enzymes was achieved through the synthesis of functional

311 polymeric micelles that collectively potent towards the hydrolysis of cellulose known as
312 cellulosomes. The one-pot reversible addition–fragmentation chain-transfer
313 polymerization was used for the formation of poly(styrene)-b-poly(styrene-alt-maleic
314 anhydride), followed by the usage of nitrilotriacetic acid (NTA) to attain amphiphilic block
315 copolymer. The Ni-NTA-functionalized micelles were prepared by the mixing of self-
316 assembled polymer with the solution of NiSO₄. These functionalized micelles were able
317 to synthesize core–shell nanostructures with cellulases as the immobilized biocatalyst
318 after the capturing of His6-tagged cellulases. Synergistic analysis has been achieved in
319 this study resulting from over twofold activity enhancement because of the site specificity
320 and close proximity of site particular oriented enzymes [57].

321 **2.4 Cellulases immobilization on other polymers**

322 The development of cellulase bioconjugates with N-iso propyl methyl acrylamide with N-
323 (Hydroxymethyl) acrylamide and methyl acrylate for recyclable thermo-responsive
324 immobilization support was studied by Ding et al. [58]. The process of construction of
325 bioconjugate is shown in Figure 5 [58]. Small-molecular quenching was applied for the
326 adjustments of the LCST by the aminoxy polymerization of N-isopropylmethacrylamide
327 (PNMN). PNMN by carbodiimide bioconjugate (PNMN-C) was covalently linked with the
328 cellulase. The highest immobilization yield was 83.2% for the polymer-cellulase
329 bioconjugate construction under the optimized conditions. The free cellulase revealed the
330 maximum activity at 55.0 °C (pH 5.0) as compared to the polymer-cellulase bioconjugates
331 at 50.0 °C (pH 5.0). After repeated five hydrolysis experiments, 85.2% of initial activity
332 was maintained for polymer-cellulase bioconjugate. As compared to the LCST, PNMN
333 could be collected as precipitate after dissolving and efficient use at 50.0 °C [58].

334 The impactful carriers favorable for the cellulase immobilization were investigated by Tata
335 et al. [59] by free radical cross-linking co-polymerization in reverse suspension to prepare
336 the copolymers of divinylbenzene (DVB) and N-vinylformamide (NVF). The variation of
337 spherical and crosslinking nanoparticles with variable sizes were used for the synthesis
338 of nanocarriers types based on P(NVF-co-DVB). The three (VAM-co-DVB) polymers with
339 vinylamine units were achieved after the hydrolysis of the formamide carrier group into
340 the amino groups. The vinyl formamide groups (without glutaraldehyde) and VAM (with
341 glutaraldehyde) were used for cellulase immobilization. The efficient immobilization of

342 cellulase was achieved by tested carriers that act as excellent support materials. But as
343 compared to the native enzyme, the enzyme immobilized on the P(VAM-co-
344 DVB0.27)/2000/350 carrier showed the highest catalytic activity [59].

345 The production of cellulose-derived bioethanol was studied by cellulase enzyme
346 immobilization to enhance the catalytic productivity and cellulase reusability [60]. The
347 visible light induced graft polymerization on low-density polyethylene films, fabricated by
348 a layered structure with a thin poly(ethylene glycol) gels as the inner layer and sodium
349 polyacrylate (PAANa) brush as the outer layer. This hierarchical support showed for the
350 immobilization of two enzymes i.e., cellulase and β -glucosidase. The β -glucosidase from
351 the LDPE surface was *in situ* entrapped into inside hydrogels layer during the polymeric
352 grafting to improve the catalytic efficiency additionally to cellulase. The cellulase was
353 covalently immobilized on to the outer PAANa brush layer during the reinitiating of sodium
354 acrylate after its polymerization on the PEG hydrogel layer. The β -glucosidase could
355 attain the high activity after the graft polymerization because of the slight reaction such
356 as visible-light irradiation. The optimal temperature of cellulase and the β -glucosidase or
357 the optimal pH did not change during the immobilization. But after the immobilization, the
358 sudden shift of pH 5.0 was observed in case of cellulase. The dual enzyme system
359 showed the 82% and 20% enhanced enzymatic efficiency contrasting with the original
360 activity of isolated BG/cellulase immobilization system and single cellulase system. The
361 repeated experiments up to 10 cycles of CMC hydrolysis relative to original activity shows
362 high stability and recyclability of enzyme after immobilization [60].

363 **3. Cellulases immobilization on nanosupports**

364 **3.1 Cellulases immobilization on silica-based supports**

365 The electrostatic interaction is an important factor to consider for the intensification of
366 adsorption rate, while dealing with immobilized cellulases and other enzymes. Therefore,
367 the development of opposite surface charges on the enzyme and the carrier is considered
368 as basic factor [61]. Secondly, the adjustment of pore size for the entrapment of enzymes
369 is essentially must not be so large that it will cause desorption. Therefore, the similarity is
370 necessarily required in the mesopores size and the molecular dimensions of the
371 biocatalysts [25,62]. Cellulases exhibit high affinity with hydrophobic surfaces, therefore,
372 the hydrophobic groups of silica surfaces also have significant role in enzyme adsorption

373 and desorption. Poorakbar et al. [63] developed mesoporous silica-magnetic Au-NPs
374 core-shell for the immobilization of cellulase enzyme. Santa Barbara Amorphous-15
375 (SBA-15) was used for the early immobilization of cellulase on mesoporous silica-based
376 nano-support [64,65]. The accommodation of bulky enzymes was carried on the SBA-15
377 because of its larger pores size. Takimoto et al. [66] studied the cellulase produced from
378 *Trichoderma viride*, immobilized on SBA-15 nanosupports with different pore sizes of 4,
379 8.9, and 11 nm. The SBA-15 (isoelectric point (pI) = 3) was negatively charged and the
380 cellulase (pI = 4.9) was positively charged. The electrostatic interactions were considered
381 as the driving force for the enzymatic adsorption on nano-supports [66]. The
382 measurements were taken at pH 4.0 and 37 °C for cellulase activity determination based
383 on the hydrolysis of crystalline cellulose. The highest activity was reported by the use of
384 intermediate pore sized support, regardless of conviction that the largest pore size
385 support indicated the smallest increase in the amount of absorbed enzyme. The smaller
386 pores of silica were not enough to penetrate the large microcrystalline cellulose. The
387 cellulase was primary entrapped in the interior of the pores (11 nm sized) support,
388 however, in case of .9 nm pore size, the cellulase molecules were located at or very close
389 to the entrance of the pores. The immobilized nanobiocatalyst showed improved storage
390 stability and recyclability [66].

391 Hartono et al. [67] studied the immobilization of cellulase *via* physical adsorption using
392 organo-operational FDU-12 type mesoporous silica-based supports. The immobilization
393 showed favorable behavior towards FDU-12 materials with larger pore size and high pore
394 connectivity. However, the desired interaction between enzyme and silica support was
395 achieved by surface modification through selective functionalization. This development
396 was carried out by the co-condensation of organosilanes (trimethylbenzene), vinyl-
397 (VTMS) trialkoxysilane, 3-mercaptopropyl (MPTMS), 3-aminopropyl- (APTES) and
398 TEOS. S-APTES and S-VTMS were selected for further studies. The loading capacity of
399 S-APTES (21.80 mg/g) was higher than the S-VTMS (18.19 mg/g). While, the FDU-12
400 had the 10.35 mg/g of support loading capacity, which was less than both functionalized
401 nanocomposites. The adsorption pH 4.8 gave the negative charge to the support matrices
402 and the enzymes which contributed to the loading capacity of S-VTMS to provide the
403 hydrophobic interactions between the vinyl group and the enzyme. The CMC hydrolysis

404 revealed higher activity retention (up to 70% of the free enzyme) for S-VTMS, while the
405 S-APTES showed less activity (3.4%) of the free enzyme. The formation of amide bonds
406 at the enzyme active site imparted less S-APTES activity due to the active site of cellulase
407 which contained these residues. The benign microenvironment for cellulase activity was
408 developed due to the presence of hydrophobicity in S-VTMS. The S-VTMS reattained
409 100% of its initial activity after 15 days with very minute leaching [67].

410 Harmoko et al. [68] investigated the co-condensation optimization of tetraethyl
411 orthosilicate (TEOS) and conc. vinyltrimethoxysilane (VTMS) in term of particle size for
412 cellulase immobilization. The nano and micro particles were synthesized by varying the
413 VTMS/TEOS ratio along with pore entrance of 5-6 nm and pore size of 9-10 nm. This
414 study revealed the higher activity for the cellulase immobilized on silica nanoparticles in
415 contrast to microparticles with immobilized cellulase. This feature was explained by higher
416 microparticle channel length that caused the inactivity of enzyme. The efficient contact
417 between enzyme and substrate was observed due to the short channel length of
418 nanoparticles which prevent the formation of inactive site along the pore channels [68].

419 Similarly, Chang et al. [69] developed silica nanoparticles of ultra large pore (20–40 nm)
420 and small pore size of 2-5 nm. Dimethyl phthalate as pore expander was utilized for the
421 formation of larger pore sized materials by co-condensation with 3-
422 aminopropyltrimethoxysilane. They immobilized the enzyme on large porous silica by
423 both physical adsorption and covalent binding. The functionalized silica was prepared by
424 covalent crosslinking of cellulase to (3-trietoxysilylpropyl) succinic acid anhydride (TESP-
425 SA). High immobilization efficiency was reported by large pore sized silica as compared
426 with smaller pore size. The presence of both Si-OH and Si-NH₂ groups provided the larger
427 pore size to the silica supports than cellulase molecule size. Therefore, electrostatic
428 interaction between cellulase and Si-NH₂ enabled easy physical adsorption [69].

429 The ionic liquid method was applied to synthesize the oligomers of cellulose. The glucose
430 yield of free cellulase was approximately 85% which plotted further against the glucose
431 yields of the three biocatalysts were 33.30%, 77.89%, and 83.79%, respectively. The
432 importance of pore size of the host material was proved by the results [70]. The carboxylic
433 groups showed the binding with the cellulose-binding domain. The covalent crosslinking
434 was shown by the storage stability of TESP-SA that hinder enzyme leaching, however, it

435 showed 86.56% of glucose yield after 23 days' storage at room temperature. The direct
436 linkages between carboxylic acids possibly present in the active site of the enzyme and
437 $-NH_2$ of APTES was avoided by the operated silica-surface with APTES, followed by
438 glutaraldehyde crosslinking. The steric constraints are avoided by the glutaraldehyde
439 acting as a spacer arm between the matrix and the enzyme. In another study, Kannan
440 and Jasra, [71] studied the *Penicillium funiculosum* cellulase immobilization on meso-
441 cellular foams *via* covalent linking. The operated reactions was consisted of APTES with
442 amino functionalization and glutaraldehyde crosslinking. The pore size was decreased
443 from 21.8 nm to 10.8 nm by the crosslinking of meso-cellular foams; however, the pores
444 had sufficient vacuum for cellulase shelter. The modified meso-cellular silica with surface-
445 functional groups for CMC hydrolysis was shown with greater activity of the immobilized
446 enzyme. Furthermore, the immobilized enzyme showed higher V_{max} (9.8 U/mg) in contrast
447 to free enzyme (5.3 U/mg). The enzyme and meso-cellular silica surface revealed
448 opposite charges at pH 5. However, the diffusion of substrate molecules and enzyme was
449 easy due to larger pore size. Moreover, 66% of the initial activity was retained after 15
450 reaction cycles which exhibited excellent stability of immobilized cellulase [71].
451 Yin et al. [72] studied the immobilization of cellulase enzyme using mesoporous silica
452 (SBA-7) as support material without the $NaBH_4$ reducing. They found 8-fold increase in
453 V_{max} assigned to the stability enhancement after immobilization. Limited substrate
454 diffusion was observed inside the pores due to increased K_m value. The support materials
455 maintained the enzymatic tertiary structure at high temperature. The multi-point
456 attachment caused the higher activity of immobilized cellulase in broad range of pH and
457 increase in thermal stability at 60 °C. After 11 cycles of reaction, the 88% of initial activity
458 was conserved for immobilized cellulase. Similarly, Zhang et al. [73] studied
459 immobilization of cellulase on silica gel by covalent linking. Herein, the used surface
460 functionalization reduced the industrial-silica pore size from 10.6–16.2 nm to 7.7–10.6
461 nm. The loaded cellulase retained 7% of its initial activity in CMC hydrolysis with quantity
462 of 18.8 mg/g of silica gel. The activity loss was observed in three steps during reuse for
463 immobilized enzyme. The 82-100% of activity was reattained from 1st to 7th cycle, 60-
464 48% from 8th to 13th cycle, and 23-36% from 14th to 26th cycle. It was observed that the
465 enzyme desorption by support caused decomposition of outer surface and denaturation

466 in the vicinity of the pores at the 2nd stage. The conformational structure shifting was
467 reported to protect the cellulase inside the pores. The storage of immobilized enzyme at
468 4 °C for 32 days retained the 92.4% of its initial activity and high storage ability [73].
469 Ungurean et al. [74] studied *Trichoderma reesei* cellulase immobilization using binary and
470 tertiary mixtures of tetramethyl orthosilicate (TMOS) with methyl-(MeTMOS), and phenyl-
471 trimethoxysilane (PhTMOS) for the development of nanobiocatalyst using sol-gel
472 encapsulation method. MeTMOS/TMOS with 3:1 molar ratio and no additives were used
473 to derive the best operating materials at 4.8 pH in CMC hydrolysis experiment. This study
474 reported more than 90% of total enzyme recovery. The hydrolysis of microcrystalline
475 cellulose (Avicel PH101) was used to study the catalytic efficiency of the entrapped
476 enzyme. The decrease of the kinetic nature was observed by immobilized enzyme and
477 longer reactions; however, after 24 h reaction, the immobilized enzyme showed the less
478 glucose yield than the free one. The immobilized enzyme showed the 10–20% higher
479 thermal stability as compared to free cellulase and increase in pH stability was observed
480 in the pH domain 5.5–7.0. The rigidity provides the protection against undesirable
481 modifications by preventing the denaturation and microenvironment inside the porous
482 structure. An enhancement of enzyme/substrate affinity was used to explain the half K_m
483 for the immobilized cellulase as compared to free one. The mass transfer resistance
484 within the sol-gel matrix showed threefold decrease in V_{max} . The 20% leaching after the
485 6th cycle described the effective reusability potential for various applications [74]. Chen
486 et al. [75] studied the synthesis of two mesoporous silicates having pore size of 3.8 and
487 17.6 nm, and the cellulase immobilization was performed by pure physical adsorption
488 method. The pore size of the mesostructured support was associated with the enzyme
489 loading. The 1.2-times higher cellulase loading was observed for MS-17.6 pore size.
490 Some cellulase molecules of MS-3.8 played role in blocking the pore entrance. However,
491 the cellulase molecules were easily well managed and adjustable into the MS-17.6 due
492 to larger space. The opposite trend with respect to loading was observed during the
493 measurement of activity of the two biocatalysts, in the CMC hydrolysis at 50 °C and pH
494 5.0. The MS-17.6 showed the less specificity of 26.6% as compared to the MS-3.8
495 displayed a higher specific activity (63.3% of free cellulase). The MS-3.8 was observed
496 to increase the availability of active site, trapping of molecules in the pore entrance and

497 conserving the native structure of cellulase. The conformational flexibility of cellulase
498 lowered its activity because of the obstruction caused by the dense and ordered
499 arrangement of MS-17.6. However, the interaction of substrate with the enzyme require
500 the conformational change [75].

501 **3.2 Cellulases immobilization on non-magnetic magnetic nanostructures**

502 Different methodologies have been designed to gain wide range of enzymatic applications
503 following low toxicity, enzyme recovery, excellent separation from the reaction mixture,
504 and improved stability for cellulase immobilization on magnetic nanoparticles (MNPs).
505 The cellulase immobilization on MNPs was proceeded by both the nonspecific physical
506 adsorption and covalent binding [20]. Different binding types have been observed such
507 as hydrophobic or stacking interactions, van der Waals, and electrostatic forces during the
508 enzyme's interaction with the surface of nanomaterials by non-covalent binding [76]. The
509 protein leakage from the surface of nanomaterial was observed as the major drawback
510 from the non-covalent immobilization. The leakage from the carrier and high operational
511 stability was observed during the covalent binding of enzymes [77]. The nanomaterials
512 characteristics such as size, functionalization and structure greatly influence the catalytic
513 behavior and stability of cellulase to determine the effect of magnetic nanoparticles [78].
514 The conformation and biological function of conjugated enzymes, adsorption effect, and
515 nanomaterial interaction with protein molecules are greatly influenced by the surface
516 chemistry of these nanomaterials [79]. For example, aiming to increase the enzymatic
517 stability, the immobilization was performed on superparamagnetic nanoparticles through
518 ionic linking [80]. Figure 6 shows cellulase immobilization onto iron oxide nanoparticle
519 surfaces [78].

520 In different experiment to increase the magnetization of nanoparticles and saturation, an
521 activated magnetic support using zinc doping was applied for cellulase immobilization by
522 Abraham et al. [81]. The loading of the enzyme was increased by series of porous
523 terpolymers with crosslinking through suspension and polymerization [82]. In a recent
524 study, Abbaszadeh and Hejazi, [83] immobilized *Aspergillus niger* cellulase using amine
525 functionalized Fe₃O₄ magnetic nanoparticles *via* metal binding affinity immobilization. The
526 nano-biocatalytic characterization was performed for the cellulase immobilization by the
527 addition of any intermediate, and copper was selected as ligand for enzyme loading on

528 magnetic nano-supports in buffering surroundings. The relative enzyme activity 91% was
529 determined, and the amount of enzyme 164 mg/g of magnetic nano-supports, under the
530 optimized conditions. The immobilized enzyme exhibited more stability than free enzyme
531 tested by CMC hydrolysis at 1% concentration. Moreover, after five cycles of reusability,
532 immobilized enzyme reattained 73% of its initial activity. After 8 days of storage at 4 °C,
533 the immobilized cellulase reattained 84% of their initial activity and 70% of initial activity
534 for free cellulase [83].

535 Mo et al. [84] studied the cellulase immobilization using porous biochar-based support
536 material obtained from lignocellulose biomass due to its attractive properties i.e., poly-
537 porous structure and high specific surface area. The preparation of γ -Fe₂O₃ combined
538 with poly-porous biochar was performed by calcination which was used as support
539 material for the immobilization of cellulase. The highest immobilization capacity (266
540 mg/g) was achieved for cellulase immobilization with relative 73.6% activity as compared
541 with free enzyme. The results indicated that by increasing temperature, endothermal
542 process was occurred, which resulted high cellulase adsorption. Similarly, Paz-Cedeno
543 et al. [85] studied the immobilization of cellulase and xylanase enzymes using graphene
544 oxide-magnetic nanoparticles (GO-MNPs) as support-material for efficient synthesis of
545 cellulosic ethanol and other useful compounds. Homogeneous distribution of MNPs onto
546 the graphene oxide nanosheets was observed. The nanobiocatalysts were developed by
547 covalent crosslinking using hydroxysuccinimide and 1-ethyl-3-(3-
548 dimethylaminopropyl)carbodiimide. The designed nanobiocatalyst showed enhanced
549 efficacy for sugarcane bagasse hydrolysis and showed relative activities 66%, 70%, 70%,
550 88% after ten consecutively repeated experiments for xylanase, β -xylosidase,
551 endoglucanase, and β -glucosidase, respectively. The 80% and 50% nanobiocatalysts
552 efficiency was reported for cellulose and xylan hydrolysis, respectively. The results
553 indicated it as a potential candidate for cellulosic ethanol production.

554 **3.3 Cellulases immobilization on cross-linked enzyme aggregates**

555 The attractive concept that offers valuable technology is explained by the cross-linked
556 enzyme aggregates (CLEAs). Potential advantages of CLEAs are shown in Figure 7 [86].
557 Generally, the procedure of making CLEAs include physical precipitation followed by
558 glutaraldehyde crosslinking [87,88]. The resulting CLEAs exhibit improved enzymatic

559 activity and recyclability up to several folds than native enzyme [89]. However, the
560 optimum recovery and handling of CLEAs is difficult because they are mechanically
561 fragile [90]. Kim et al. [91] reported the formation of CLEAs entrapped in mesoporous
562 silica, which did not show leaching through narrow channels. Moreover, significantly high
563 enzyme loading, and improved activity was reported after CLEAs immobilization. The
564 one-pot bioconversion of lignocellulosic biomass to fermentable sugars was achieved
565 through the preparation of CLEAs with xylanase, cellulase and β -1,3-glucanase [92]. The
566 development of CLEAs was carried out by three-phase partitioning (TPP) method. The
567 crosslinking time of 7.5 h was given with glutaraldehyde (100 mM) as a chemical
568 crosslinker. The initial 70% of activity was reattained at 70 °C compared to 30% for the
569 free enzyme indicating good thermal stability of CLEAs. After the incubation for 11 weeks
570 at 4 °C, more than 97% of activity was observed indicating excellent storage stability of
571 CLEAs in contrast to 65% of initial activity for free enzymes. The reuse of CLEAs was
572 made possible due to the presence of free enzymes in the hydrolysate inhibiting their
573 restoration. The CLEAs caused the maximum hydrolysis of ammonia about 83.5% in 48
574 h while the free enzymes hydrolyzed the sugarcane bagasse about 73% [92]. Similarly,
575 Perzon et al. [93] studied the formation of cellulase-CLEAs *via* precipitation and
576 crosslinking method which proved as rapid and multifunctional way. There is still needed
577 to elucidate the association between the process parameters and cellulase-CLEA final
578 activity. The CLEAs made from cellulase (EC 3.2.1.4) were optimized for various factors.
579 The different temperature, crosslinking time, and crosslinking concentrations were used
580 for three types of participants such as ammonium sulfate, polyethylene glycol, tert-butyl
581 alcohol. The polyethylene glycol and ammonium sulfate-CLEAs were recovered 29% and
582 17% of the free enzyme activity, respectively. However, the CLEAs synthesized with tert-
583 butyl alcohol were inactive. The ammonium sulfate-CLEA only recovered 10% of its
584 activity after one cycle whereas the polyethylene glycol-CLEA recovered 40% of the initial
585 activity after four cycles which demonstrated the significance of precipitant on final CLEA
586 activity instead of enzymatic activity in re-solubilization. The ammonium sulfate showed
587 better performance in CLEAs while PEG was not capable to precipitate enzyme [93].
588 In another study, the supercritical carbon dioxide was used for the activation of cross-
589 linked cellulase aggregates by Podrepšek et al. [94]. Several precipitating reagents such

590 as propanol, tetrahydrofuran, 2-propanol, acetone, ammonium sulphate, ethanol, and
591 methanol were used to analyze the enzyme precipitation. The highest enzyme activity
592 was achieved by the immobilized enzyme using optimized enzyme concentration of BSA
593 and glutaraldehyde. This study presented the efficient and cost-effective biosynthetic
594 process using 0.0625% glutaraldehyde concentration, and precipitant ethanol. The
595 enhanced level of reusability and stability of immobilized cellulase was reported. This
596 study also indicated more catalytic sites on spherical structure of CLEAs with high surface
597 area. The introduction of new catalytic sites proved beneficial for the nanobiocatalyst [94].
598 Due to increased depletion of fossil fuels, an alternative energy production way was
599 investigated using enzymatic conversion methodologies using renewable biomass
600 resources and formation of high-value chemicals are being promoted [95-100]. The
601 efficient pH and thermal stability, and recyclability have been reported by the enzymes
602 after immobilization. Jia et al. [101] studied the novel magnetic CLEAs development for
603 the immobilization of cellulase. High thermal and pH stability was observed by the CLEAs
604 immobilized enzyme as compared to free enzyme. The immobilized cellulase maintained
605 the 74% of its initial activity along with the successful magnetic separation after the
606 continual six repeated cycles of CMC hydrolysis. The immobilized enzyme showed the
607 high potential for biomass conversion, indicated by reusability (38% activity retention) up
608 to 4 cycles of biomass conversion and 21% yield during the hydrolyze of bamboo biomass
609 [101].

610 Jafari Khorshidi et al. [102] conducted study on the amine-functionalized Fe_3O_4 @silica
611 core-shell magnetic nanoparticles for the immobilization of cross-linked aggregates
612 (CLEAs) of cellulase aiming to increase usability for the industrial bioconversion of
613 lignocellulosic materials to glucose and other renewable biomaterials. The significant
614 change was not observed in optimum temperature during the acidic behavior switched by
615 the optimum pH of the cellulase cocktail upon immobilization (cellulase CLEA-MNP). The
616 free cellulase lost all of its activity while the cellulase-CLEAs-MNP maintained about 45%
617 of its initial activity. However, at 80 °C, immobilized cellulase maintained 65% of highest
618 activity than the free enzyme. The highest thermal stability was developed at 65°C.
619 Cellulase CLEAs-MNP reattained 30% of its initial activity through six cycles of reusability
620 after the acute decrease during two cycles of CMC hydrolysis [102]. Similarly, Li et al.

621 [103] synthesized a new carrier-free cross-linked aggregates of cellulase (CLEAs-C)
622 through $(\text{NH}_4)_2\text{SO}_4$ precipitation and glutaraldehyde crosslinking. As a precipitant, 95%
623 of ammonium sulfate was used to prepare cellulase-CLEAs. The 50 mg/mL cellulase
624 concentration and 3% (v/v) glutaraldehyde was used in order to acquire the excellent
625 enzymatic activity. The optimum temperature was found to be 60 °C, while the pH 3.0
626 was found most effective. The CLEAs maintained the 80% of initial activity during the
627 storage for 28 days at 4 °C [103].

628 **3.4 Cellulases immobilization on metal oxide nanoparticles**

629 Different kinds of metal oxides (TiO_2 , ZnO, $\text{Fe}_2\text{O}_3/\text{Fe}_3\text{O}_4$, Bi_2O_3 , CeO_2 , SiO_2 , MoO_2) are
630 important for various applications including usability in gas sensors, dye sensitized solar
631 cells, and their catalytic, antimicrobial, electronic, electrical conductivity, and high optical
632 characteristics [104-106]. However, the high cost and environmental factors influence the
633 recovery and reusability of nanostructures. Therefore, immobilization and incorporation
634 are carried out by distinct type of substrates but finding of an appropriate substrate is still
635 a major concern. Various metal oxide nanostructures have been immobilized due to its
636 natural biopolymer properties. In paper matrices, the retention issues are resolved by
637 using the retention aids, binders, and appropriate linkers to conduct the immobilization
638 and incorporation [107,108]. The use of metal oxide nanoparticles for catalytic
639 immobilization purpose have widely been investigated [108-110]. For instance, Jordan et
640 al. [109] studied the immobilization of cellulase enzyme onto magnetic iron oxide (Fe_3O_4)
641 nanoparticles *via* carbodiimide activation and covalent binding. After the binding of
642 complex, no significant change in size was observed in the magnetic particles, and SEM
643 micrographs revealed a mean diameter of 13.3 nm. Enzyme was supported on the
644 saturation point occurred at a weight ratio of 0.02 and low enzyme loadings demonstrated
645 the maximum binding of 90%. The relative peak enzyme activity was analyzed at 50 °C
646 and enhanced stability was observed over the boarder range of temperature by thermal
647 measurements of nanoparticles. The shift in optimum pH from 4.0 to 5.0 was observed
648 by the ionic forces between the enzyme and support surface [109].

649 Xu et al. [111] studied cellulase immobilization on magnetic Fe_3O_4 nanoparticles through
650 glutaraldehyde crosslinking. No structural or particle size changes were observed by
651 binding step, and the mean diameter of 11.5 nm was observed in all the nanosized

652 particles of the magnetic particles with or without bound cellulase. The covalent binding
653 was observed between residual amine groups on magnetic Fe₃O₄ nanoparticles and
654 amine groups of the cellulase efficiently controlled the binding capacity of cellulase. As
655 compared to the free enzyme, improved storage stability and wider ranges of pH and
656 temperature was observed by immobilized cellulase. Immobilized cellulase showed the
657 greater affinity for cellulosic substrate than the free enzyme determined by the enzyme
658 kinetics. The hydrolysis of steam-exploded corn stalks and bleached sulfa the bagasse
659 pulp demonstrated the efficient performance for the immobilized cellulase [111]. Han et
660 al. [112] conducted a study for cellulase immobilization using the surface of magnetic-
661 Fe₃O₄ nano-supports modified by dendritic polymer 4-arm-PEG-NH₂. The covalently
662 immobilized cellulase was prepared by the glutaraldehyde that act as coupling agent for
663 the magnetic supports. Different characteristics such as reusability, storage stability,
664 optimum temperature, Michaelis constant, thermal stability and PH were analyzed.
665 Results indicated 132 mg/g loading ability of cellulase with wider range of pH,
666 temperature, storage, and functional stability as compared to the free cellulase. The 76%
667 increased catalytic activity was observed by immobilized cellulase as compared to the
668 free cellulase [112].

669 Abbaszadeh and Hejazi, [83] conducted metal affinity immobilization of cellulase on the
670 amine functionalized Fe₃O₄ magnetic nanoparticles (MNPs). The process was carried out
671 without any addition of intermediates, and copper was chosen as ligand and loaded on to
672 magnetic nanoparticles in buffering solution. The relative enzyme activity (91%) was
673 reported, and the amount of immobilized enzyme was 164 mg/g of MNPs under optimized
674 conditions (Cu/MNPs = 1, E/MNPs = 0.11, pH = 6). In contrast to the free enzyme, the
675 immobilized cellulase showed more stability tested by repeated CMC hydrolysis at 1%
676 concentration. Furthermore, 73% of initial activity of immobilized cellulase was reattained
677 after the 5 cycles of usability. The storage step at 4 °C showed the 70 and 84% of initial
678 activity for free and immobilized cellulase after the 8 days storage. This study proved as
679 an excellent candidate for various biotechnological and industrial sectors [83].

680 **3.5 Cellulases immobilization on carbon nanotubes/nanorods**

681 Different strategies have been applied for the synthesis of nanotubes of transition metal
682 chalcogenide materials such as the chemical vapour deposition, use of solid templates

683 and chalcogenization, etc. Carbon nanotubes formed by such transition metal
684 chalcogenide materials are maybe single walled (SWCNT) or multi walled (MWCNT).
685 Significant research has been conducted to immobilize biocatalysts on these carbon
686 nanotubes and nanoroads. For instance, Mubarak et al. [113] studied the immobilization
687 of cellulase enzyme on functionalized-MWCNT using physical absorption process to
688 overcome the catalytic stability and efficiency issues. The optimum enzyme
689 immobilization percentage of 97% was attained by the usage of 4 mg/mL enzyme
690 concentration. The optimum reaction conditions were reported as 50 °C temperature and
691 pH 5. Characterizational results indicated high efficiency of nanobiocatalyst because
692 cellulase-MWCNT nanocomposite retained 52% of its initial activity after six repeated
693 experiments of CMC hydrolysis. The convenient separation and high stability make it a
694 robust candidate for various applications [113].

695 Ahmad and Khare, [114] reported the immobilization *Aspergillus niger* cellulase onto
696 functionalized-MWCNT by carbodiimide crosslinking. MWCNT impart useful
697 characteristics including rapid electrode kinetics, high edge-to-plane ratio, enhanced
698 electronic properties and improved tensile characteristics because of structural
699 arrangements. The nanobiocatalyst designed under optimized conditions exhibited high
700 thermal and pH stability, with up to 85% activity retention. The half-life of nanobiocatalyst
701 was 4-folds higher than free enzyme at 70 °C temperature. Two folds increase in K_m value
702 of resulted nanobiocatalyst towards the substrate was reported. High reusability potential
703 was reported by 10 consecutively repeated experiments without much actual enzymatic
704 activity loss, which make it potential candidate for effective cellulose hydrolysis. Similarly,
705 Ma'an et al. [115] studied the production of cellulase from *Trichoderma reesei* and the
706 enzyme was immobilized on functionalized-MWCNTs *via* covalent crosslinking. Different
707 parameters were optimized to get efficient immobilization yield which indicated three most
708 influential parameters i.e., temperature, pH, and EDC concentration. The optimized
709 conditions were 30°C temperature, 4.5 pH, and 1 mL (10 mg/mL) of EDC. The highest
710 immobilization yield (98%) was achieved using above-mentioned optimized conditions
711 [115].

712 Li et al., [116] reported novel method for immobilization of cellulase using combined
713 sodium alginate and MWCNT. The optimizational results indicated temperature 40 °C and

714 pH 3.0. Cellulase activity retention (71.2% of its initial activity) was reported after 1 month
715 of storage at 4 °C temperature. The nanobiocatalyst showed up to 70% of its initial activity
716 after 7 consecutively repeated experiments of cellulose hydrolysis. Moreover, high
717 thermal and pH stability, storage stability, and recyclability was reported which showed
718 potential for biotechnological applications. Similarly, Azahari et al. [117] reported cellulase
719 production from *Trichoderma reesei*, and its successful immobilization was performed
720 using MWCNTs by physical absorption. The nanobiocatalyst showed enhanced pH and
721 thermal stability profiles as compared with free cellulase at pre-optimized conditions of
722 pH 5 and temperature 50 °C. After consecutive 3 experiments up to 60% of cellulase
723 activity retention was demonstrated by nano-conjugates [117]. The easy separation, high
724 thermal and pH stability, and excellent reusability of CNT immobilized enzyme make them
725 robust catalyst for various biotechnological and industrial applications.

726 **3.6 Cellulases immobilization on graphene oxides nanoparticles**

727 Cellulase immobilization was performed by the development of graphene-based nano-
728 supports with controlled pH and temperature and magneto-responsive properties [118].
729 The 2D immobilization supports created the issue of geometric drawback which was
730 resolved by the synthesis of closed copied free functionalized biocatalyst under similar
731 reaction environment. The covalent immobilization showed the betterment in the bio-
732 receptivity of graphene supports and supramolecular assembly of oppositely charged
733 quenched polyelectrolytes and maghemite–magnetite nanoparticles on 2D graphene
734 supports. The chances of recovery and reuse of the enzyme over multiple cycles were
735 achieved by the incorporation of magnetic nanoparticles. The 55% of initial activity was
736 exhibited by immobilized enzymes after four repeated experiments. The effective tool to
737 control the activity of immobilized enzymes was achieved through the modified degree of
738 polyelectrolyte swelling by the controlled temperature and pH. In contrast to the
739 immobilized enzymes without the brushes, the immobilized enzyme with stiffed
740 polyelectrolyte brushes showed the 1.5-fold betterment in the activity at pH 5.1 and 50 °C
741 temperature [118].

742 Gao et al. [119] used the etherification and diazotization for the synthesis of functionalized
743 graphene oxide and implantation with hydrophobic spacer P-β-sulfuric acid ester ethyl
744 sulfone aniline. The immobilization of cellulase through covalent bonding was attained by

745 the functionalized graphene oxide as a nano-support. The high immobilization yield and
746 efficiency of above 90% were observed after the optimization of reaction parameters. The
747 significant betterment was observed in thermal and functional stabilities of immobilized
748 cellulase as compared to the free cellulase. The increase of six-fold higher thermal
749 stability was observed by immobilized enzyme (533 min) in contrast to the half-life of free
750 cellulase (89 min) at 50 °C. Furthermore, the immobilized cellulase showed the highest
751 catalytic activity due to linkage between substrate and immobilized enzyme ($K_m = 2.19$
752 g/L) as compared to the free cellulase ($K_m = 3.84$ g/L). Similarly, Dutta et al. [119] used
753 the graphene oxide as nano-support reinforced with magnesium oxide nanoparticles
754 (MgN). The *Bacillus subtilis* cellulase was immobilized on GO nano-support crosslinked
755 with glutaraldehyde which increased 3.5-folds increase in enzyme activity at 90 °C and
756 2.98-folds increase in enzymatic activity at 8 °C. In contrast to the untreated enzyme, the
757 MgN-cellulase graphene oxide showed 5-folds and 4.7-folds increase in V_{max} at 8 °C and
758 90 °C and 6.7-folds decrease in K_m at 8 °C and 34-folds at 90 °C was reported. In contrast
759 to the natural enzyme, GO-MgN-cellulase showed the half-life of 41.6-folds at 8 °C while
760 72.5-fold half-life at 90 °C. The storage stability of GO-MgN-cellulase was observed at 4
761 °C for more than 120 days and the enzymatic activity was maintained even after 12
762 repeated uses [119].

763 Paz-Cedeno et al. [85] studied the immobilization of cellulase on magnetic graphene
764 oxide nanoparticles (GO-MNP) as support-material. The immobilized biocatalysts were
765 designed by carbodiimide crosslinking. The developed nanobiocatalyst showed
766 enhanced efficacy for sugarcane bagasse hydrolysis and showed relative activities 66%,
767 70%, 70%, 88% after ten consecutively repeated experiments for xylanase, β -xylosidase,
768 endoglucanase, and β -glucosidase, respectively. The 80% and 50% nanobiocatalysts
769 efficiency was reported for cellulose and xylan hydrolysis, respectively. The results
770 indicated it as a potential candidate for cellulosic ethanol production. Similarly, Zhang et
771 al. [120] studied the co-immobilization of glucose oxidase and cellulase using graphene
772 oxide as support-material. The one-pot modification of gluconic acid from CMC due to
773 feasible control of loading enzymes with different sorts was reported. The multi enzyme
774 systems had the superficial pH 5 and temperature 40 °C. The values of kinetic constants
775 were $V_{max} = 0.18 \pm 0.01 \mu\text{mol}\cdot\text{L}^{-1}\text{s}^{-1}$, $K_{cat}/K_m = 24.12 \pm 0.52 (17.74 \pm 0.85) \text{s}^{-1} \text{mmol}^{-1}\text{L}$ and

776 $K_m = 0.15 \pm 0.02$ (0.43 ± 0.09) mmol.L⁻¹. The loading abilities of cellulase and glucose
777 oxidase on nanobiocatalyst were 49.07 ± 7.47 mg/g and 10.22 ± 2.03 mg/g. After seven
778 cycles, almost 65% of the initial activity was reattained by immobilized catalysts.
779 Remarkably, the $63.82 \pm 8.03\%$ conversion of gluconic acid was observed within 2 h of
780 treatment [120].

781 **3.7 Cellulases immobilization on nanostructured hybrid organic-inorganic** 782 **nanosupports**

783 There has been a growing interest in designing hybrid organic-inorganic nanosupports
784 for potential applications in biocatalytic immobilization with the aim to improve recyclability
785 and stability for bioprocessing applications [121,122]. The development of organic-
786 inorganic hybrid nanostructure is quite convenient, but it requires up to three days, which
787 restrict their workability. Therefore, Batule and coworkers designed a sonochemical
788 method, which can rapidly (within 5 min) synthesize organic-inorganic hybrid nanoflowers,
789 apparently due to sonication method causing quick self-assembly of copper phosphate,
790 delivering high energy to the structure [123]. These newly designed hybrid nanoflowers
791 exhibited improved stability and recyclability with similar morphology to those synthesized
792 by conventional method. Studies have primarily reported copper ions for the synthesis of
793 hybrid nanomaterials; however, various other inorganic ions have also been used for this
794 purpose [124]. The immobilization of cellulase using TiO₂-lignin hybrid support *via*
795 physical absorption was reported by Zdarta et al, [125]. The immobilized cellulase was
796 precipitated by the physical adsorptions on the inorganic–organic hybrid matrix. Different
797 parameters were chosen for the early immobilization such as the 5 mg/mL enzyme
798 solution, 6 h process time, and pH 5. The free and immobilized cellulase were analyzed
799 and compared in terms of storage stability, impacts of pH and number of catalytic cycle
800 sequences. The thermal and chemical stability, immobilization time and amount of
801 enzyme solution were improved during this study evaluated by the dependence of
802 catalytic activity of the immobilized enzyme on the early immobilization factors. The
803 immobilized cellulase retained over 80% of its initial activity after 3 h at 50 °C and pH 6.0.
804 The free enzyme showed the half-life of 63 min while the nanobiocatalyst showed the
805 half-life of 307 min. The immobilized cellulase maintained over 90% of its initial catalytic
806 characteristics after the ten repeated cycles. This novel study illustrated the convenient

807 and excellent mode for the production of hybrid titanium dioxide–lignin material and its
808 utilization for the immobilization of cellulase as a support material. Over the several
809 cycles, this method proved as efficient way to utilize commercially without any expiration
810 of characteristics. Other biocatalysts could also apply this strategy for the immobilization
811 [125].

812 Dragomirescu et al. [126] immobilized the cellulase produced from *Aspergillus niger* by
813 the entrapment in the Na-alginate gels and in Na-alginate/silica gel-hybrid materials. Sol-
814 gel method was used to attain silica gel by using two precursors tetra ethoxy silane and
815 tetra methoxy silane. The results for the similar loadings showed that the mixed organic-
816 inorganic nano-supports showed the less CMCCase activities, as compared to the CMCCase
817 activities obtained by Na-alginate which was 1.12-1.17-times higher noticing by
818 comparing the enzymatic activities of the immobilized products. The 13% activity of the
819 cellulase was maintained after 4 cycles for the cellulase immobilized in three types of
820 aforementioned organic-inorganic gel matrices. The relative activity was 98% more than
821 the initial for the immobilized *Aspergillus niger* CMCCase after one hour of storage at 37
822 °C and pH 3.0 [126]. In addition, the immobilization of enzymes has also been studied by
823 the new type of nanomaterial known as nanoflowers that acts as novel nano-support.
824 These are hybrid in nature because of their organic and inorganic combination. The
825 organic portion is formulated by DNA and protein; however, the inorganic portion is made
826 up with metal ion such Cu, Mn, or Ca. The analytical science and catalysis have reported
827 to use the inorganic nanoflowers until the introduction of organic–inorganic nanoflowers.
828 These hybrid nanoflowers are reported to have superior features over the free or
829 immobilized enzymes due to the different properties such as higher stability and catalytic
830 activity, simple production, and greater surface area than the spherical nanoparticles. The
831 five different types of hybrid-nanoflowers are capsular nanoflowers, protein manganese,
832 copper-DNA, protein-copper, and calcium-protein nanoflowers [127,128].

833 **3.8 Cellulases immobilization on metal organic frameworks**

834 The metal organic frameworks are synthesized from the particular metal ions and certain
835 organic linkers. Further, the metal organic frameworks are species of highly ordered
836 microporous crystalline hybrid materials and identified as the porous coordination
837 polymers. Mostly used metal ions are actinide elements, alkaline-earth metals, transition

838 metals and p-block elements for the construction of metal organic framework [129]. But
839 the included organic linkers are sulfonates, carboxylates, amines, nitrates, and
840 phosphates. The magnetic organic frameworks demonstrate the unique features such as
841 plentiful binding interactions for the selection of reactant such as uniform aperture size,
842 comparatively high thermal, mechanical, and chemical stability, adjustable topological
843 structure, large particular area, intrinsic crystalline structure, adjustable ultrahigh porosity,
844 pore volumes and eximious optoelectronic characteristics (Figure 8) [130,131].

845 The development of novel cellulase immobilized magnetic organic framework composite
846 system with increased reusability and stability for cellulose hydrolysis was performed by
847 Ahmed et al. [132] using physical absorption method. The extra anchoring sites of NH₂
848 groups showed higher protein loading by NH₂-functionalized metal organic framework as
849 compared to the precursor UiO-66. Moreover, pH tolerance and increased thermostability
850 were also shown by the immobilized cellulase. The abundance of NH₂ and COOH
851 functional groups on the MOFs increase the stability of cellulase after its absorption and
852 chances of composite recovery were achieved through the mild centrifugation because
853 of the heterogeneity offered by the NH₂ and COOH groups. The maximum activity gained
854 was 85% at 55 °C while utilized at 80 °C and the residual activities were 72% after ten
855 cycles and 65% after 30 days storage. The development of cellulase-MOF composite with
856 ultrahigh operations and durability for research revealed the auspicious future by this
857 study [132].

858 Qi, Luo & Wan, [133] prepared UIO-66-NH₂ metal organic framework for cellulase
859 immobilization purposes. The highest enzymatic recovery and protein loading efficiency
860 of 78.4% was exhibited by as-prepared immobilized nanobiocatalyst. As compared to the
861 free form, the immobilized cellulase showed high catalytic efficiency, pH stability, and
862 thermal stability on the magnetic organic framework of UIO-66-NH₂. The good recycling
863 ability for 5 consecutive runs was determined by the immobilized enzyme. Moreover,
864 better tolerance towards two inhibitors (formic acid and vanillin) present in lignocellulosic
865 pre-hydrolysates was shown by the immobilized cellulase in contrast to the free one. The
866 immobilized cellulase showed 16.8% and 21.5% higher activity than free enzyme in the
867 presence of 5 g/L of formic acid and vanillin. The hydrolysis showed the betterment in
868 yield which was 18.7% and 19.6% for the aforementioned amounts of formic acid and

869 vanillin. This study suggested that the inhibitory impacts of several pretreatment inhibitors
870 on cellulase can be enhanced by the immobilization [133].

871 Zhou et al. [12] studied cellulase immobilization to attain high ionic liquid tolerance and
872 development of enzymatic hydrolysis biomass *in situ*. The study used four kinds of
873 organic metal frameworks including PCN-250, ZIF-8, UIO-66-NH₂, and MIL-100-Fe.
874 Physical adsorption method was used for immobilization. The largest enzyme adsorption
875 capacity (176.16 mg/g) was exhibited by ZIF-8 nano-supports. The activity of immobilized
876 cellulase was analyzed using CMC and filter paper as substrates in the presence of ethyl-
877 3-methylimidazolium diethyl phosphate ([Emim]DEP). As compared to the free cellulase,
878 the superior ionic liquid tolerance was achieved by the immobilized cellulase (0% to 50%,
879 v/v). The activity of the CMC and filter paper cellulase were enhanced the by 112.59%
880 and 59.86% in 50% (v/v) [Emim]DEP by the specific demonstration in ionic liquid
881 tolerance of ZIF-8-immobilized cellulase. The involved ionic liquid showed that the
882 immobilized cellulase can cause the decrease of cellulase inactivation and was linked to
883 the kinetic parameters as the immobilized cellulase had a lower equilibrium dissociation
884 constant value and a higher final enzyme plateau activity value in a reaction system. As
885 compared to the free cellulase, 50% (v/v) [Emim]DEP, the ultimate 92.92% increase was
886 observed in the ZIF-8-immobilized cellulase with *in situ* hydrolysis of bagasse [12].

887 **4. Biotechnological applications of cellulases**

888 **4.1 Applications in cellulose hydrolysis**

889 The current scenario showed the significance of lignocellulosic biomass conversion into
890 industrially useful products or biofuels. The municipal wastes, industrial waste materials,
891 and agricultural byproducts are considered as the major forms of cellulosic biomass
892 [134,135]. Bioconversion of lignocellulosic biomass to fermentable sugars by immobilized
893 magnetic cellulolytic enzyme cocktails is illustrated in Figure 9 [135]. Relevant to these
894 industries, the major concern is to eliminate these wastes from the environment. These
895 industrial wastes are converted into different forms like biohydrogen, biomethane,
896 bioethanol, and sugars with the assistance of cellulose digesting enzymes. Different
897 factors are responsible for affecting the enzymatic hydrolysis such as enzyme linked
898 factors (enzyme compatibility, product inhibition, thermal sensitivity, specificity, origin of
899 enzyme and enzyme processibility) and structural properties of solid substrate [136]. The

900 crude oil prices are indicating the increasing for the worldwide demand of fuels. The
901 facility of fossil fuel is diminishing at highest speed. The modification of lignocellulosic
902 biomass to bioethanol is possible due to the action of cellulase [137,138]. Plants have a
903 defense barrier named lignin for the enzymes to perform on celluloses. Therefore, the
904 modification of hemicellulose and cellulose biomass into smaller size sugars by the action
905 of cellulase is achieved by the pretreatment on the plants to remove the lignin from them.
906 Then fermentation is proceeded further to convert the sugars into the ethanol [139]. The
907 biomass conversion into ethanol was more conveniently obtained from *Penicillium*
908 cellulase [140]. In solid waste management, cellulase enzyme is being used to convert
909 the agricultural solid wastes into beneficial products [141,142]. The wastes lignocellulosic
910 materials are also reported to produce renewable energy sources such as bio-methane
911 and bio-hydrogen [143]. Lignocellulose hydrolysis have been showed by the immobilized
912 enzyme nearly equal to the activity obtained from free enzyme; however, high stability
913 and recyclability potential have been reported after immobilization [28]. Similarly, Ingle et
914 al. [144] studied the lignocellulosic biomass conversion by immobilized and free
915 cellulases for bioethanol production. Comparative evaluation of biomass hydrolysis from
916 both free and immobilized cellulase showed that free enzyme converted 78% cellulose to
917 glucose after 24 hours at 40 °C while, immobilized enzyme showed 72% activity in similar
918 environment. Furthermore, efficient recovery by magnetic field and recyclability up to 3rd
919 cycle was noticed which suggested 68% and 52% hydrolysis after second and third cycle,
920 respectively. These findings suggest the convenient recovery of cellulase after
921 immobilization and high reusability with improved thermal and pH stability profiles which
922 make this process useful in biotechnological sectors.

923 **4.2 Applications in pulp and paper industry**

924 The demands of paper and pulp have been enhanced by the enzyme cellulase due to the
925 different requirements of daily uses such as production of paper towels and sanitary pads,
926 bio-modification of fibers, betterment wastewater of the papermills, removing of toners
927 and ink coating from papers and for bio-mechanical pulping [145]. The woody raw
928 material along with stiffness, bulk, and high number of fines are achieved by mechanical
929 pulping such as grinding and refining of woody raw materials [146]. The downside of
930 mechanical pulping is high expenditure of energy, although the attained fibers are used

931 to produce papers of different quality. Moreover, the efficient hand sheet strength
932 properties and substantial energy savings (20–40%) are observed during refining of
933 cellulose pulping from white-rot fungi by the biochemical pulping as compared to the
934 mechanical pulping [147]. The lower degree of hydrolysis and reduce viscosity of pulp
935 were observed in endoglucanase [148]. The high productivity and trouble-free printing
936 procedure are acquired by the bio-modification of fibers that uses cellulase and
937 hemicellulose and enhances the paper sheet density and pulp beat ability [147]. The
938 recycling of waste papers such as books, magazines and newspapers can be
939 accomplished by cellulases. Thereafter, fibers could be reused in ethanol synthesis and
940 in manufacturing newspapers through bleaching. The discoloration of different sorts of
941 paper wastes have been carried out by cellulase alone or in combination with xylanases.
942 There are few benefits of enzymatic bleaching such as reduced fine particles, strength
943 enhancement, better fiber brightness and prevention of alkali [149]. Yang et al. [150]
944 reported the catalytic degradation potential of methyl orange using Ag-Pt nano-
945 constructs. The enzymatic bleaching by cellulase at acidic pH decrease the
946 environmental pollution, modification in ink particle size distribution, facilitates the
947 bleaching step and prevention of alkaline yellowing [151,152]. Yassin et al. [153] studied
948 both immobilized and free cellulases for the development of cellulose nanofibers. The
949 results indicated high thermal and mechanical stability by gel-immobilized cellulase. In
950 addition, high activity retention (85%) after six repeated experiments showed good
951 recyclability potential after immobilization. The immobilized cellulose showed high
952 potential to disintegrate cellulose into nanofibrils of diameter (15-35 nm) with varying
953 length. These results indicated high applicability for paper and pulp industry and
954 packaging industry applications.

955 **4.3 Applications in food industry**

956 In food industries cellulase are used for several purposes. The nutritive juice yield with
957 better stability and less processing time is achieved by the maximum liquefaction of
958 smashed fruit pulps which continuous crushing by macerating enzyme having cellulase
959 with pectinases and hemicellulases. The decrease in viscosity, texture and cloud stability
960 of purees and juices are upgraded by macerating enzymes [154]. The higher levels of
961 antioxidants and vitamin E is observed in olive oil extracted by macerating enzymes with

962 slower initiation of rancidness [9]. The extraction of olive oil was improved by an enzyme
963 olivex which was attained by the intermixing of cellulases and hemicellulases from
964 *Aspergillus aculeatus* along with pectinase [155]. The coloring agent production for food
965 can also be achieved by cellulase [156]. The carotenoids are responsible for providing
966 the colors for many plants from red to yellow and these are also considered as the major
967 group of coloring substances in nature. The carotenoids have continuous demand in
968 market, and they are used as food colorants due to their null toxicity, natural sources,
969 high versatility, alluring characteristics and lipo- and hydro soluble colorants [157].

970 **4.4 Applications in biofuel production**

971 Enzyme immobilization using variety of different biopolymers and nanostructured
972 materials for biofuels production using biomass hydrolysis strategies have widely been
973 reported. For this purpose, various nanomaterials including nano-porous silica, carbon
974 nanotubes, graphene, nanocomposites, nanofibers, and others provide excellent support
975 material for biocatalytic immobilization. Immobilized enzymes show high operational and
976 thermal stability, and convenient recyclability using various simple chemical and physical
977 methodologies. For biofuel production, two enzymes namely, lipases and cellulases are
978 key candidates for biofuel production through various production methodologies.
979 Environmentally friendly biomass hydrolysis can be improved in terms of reusability,
980 efficiency, thermal and pH stability using enzymes immobilization technology [25].
981 Cellulases immobilization have been studied using variety of different biopolymers and
982 nanostructured materials which have previously been discussed in section 2 and 3. For
983 biofuel production applications, cellulase immobilization has been performed on silica
984 [6,36], polymeric nanostructures [158]. Affinity-tagged cellulases were investigated for co-
985 immobilization using magnetic silicon nanoparticles doped with gold using one-pot
986 cellulose hydrolysis [159]. Approaches to enhance biofuels production in the presence of
987 cellulase are shown in Figure 10 [6].

988 **5. Challenges, prospects, and conclusions**

989 Nanobiotechnological advancements are the important part of human life, especially in
990 the field of industrial. Due to the increase in human and environmental population, nano-
991 biotechnology manipulates biomaterials to improve the product yield. Cellulase is the
992 most frequently employed enzyme that convert cellulosic biomass into monosaccharide

993 building blocks which are further used for the synthesis of value-added products e.g.,
994 biofuels. Although extensive developments have been made in the immobilization of
995 enzymes using variety of different polymeric/biopolymeric, and nanostructured supports,
996 few critical issues are needed to be addressed before the industrial-scale applications of
997 nanomaterials-immobilized enzymes. It is demanded to obtain deep acquaintance and
998 insight on the influence of nanocarriers on enzymes and other biomolecules. For instance,
999 in depth studies on structural influences on nano-constructs, type of activation agent on
1000 enzymatic loading, functionalization, orientation of bounded proteins could assist in
1001 designing the optimized enzymatic systems. Moreover, such enzymatic methodologies
1002 need to be cost-effective and highly efficient. Therefore, the major challenge for the
1003 scientists is to design and optimize novel processes with improved enzymatic stability,
1004 activity, recyclability, and cost issues, along with easy down-stream processing from the
1005 reaction mixture.

1006 The recent advancements in nanostructured immobilization methodologies have shown
1007 high potential as novel nanobiocatalysts, which can further be optimized in terms of
1008 catalytic efficiency. The re-designing and engineering of novel nanomaterial-based
1009 systems for enzyme immobilization with finely tuned functionalities and structural
1010 features, exhibiting high biocompatibility, minimal toxicity, and insignificant
1011 environmentally hazardous influences accompanied by the choice of appropriate
1012 immobilization protocol might lead to the development of functionalized nanobiocatalytic
1013 systems in the field of energy and biofuel production, biosensing, organic synthesis,
1014 biotransformation, and industrial biocatalysis [122]. The use of magnetic nanocarriers is
1015 becoming interesting due to easy enzyme separation from the reaction mixture which
1016 significantly reduce the catalytic reutilization cost. Different nanostructures having
1017 diversified functional groups as immobilization support exist i.e., inorganic-organic
1018 hybrids, silica-based, metal oxide-based, CLEAs, magnetic, carbon nanotubes (SWCNT
1019 and MWCNT), graphene oxide and others. Despite current advancements, novel
1020 methodologies are still required to achieve highly efficient nanobiocatalysts for bioprocess
1021 applications. Since the recyclability is the major concern to reduce the production cost;
1022 therefore, convenient down-stream processing without actual loss in catalytic efficiency

1023 could be the interesting research area in this regard. Studies show that immobilization
1024 have potential to impart such useful characteristics to biocatalysts.

1025 **Acknowledgments**

1026 Generous support from Khalifa University (CIRA-2020-046) is graciously acknowledged.
1027 Consejo Nacional de Ciencia y Tecnología (MX) is thankfully acknowledged for partially
1028 supporting this work under Sistema Nacional de Investigadores (SNI) program awarded
1029 to Hafiz M.N. Iqbal (CVU: 735340).

1030 **Conflict of interests**

1031 The author(s) declare no conflicting interests.

1032 **References**

- 1033 [1] Ahmed, A. A. Q., Babalola, O. O., & McKay, T. (2018). Cellulase-and xylanase-
1034 producing bacterial isolates with the ability to Saccharify wheat straw and their
1035 potential use in the production of pharmaceuticals and chemicals from
1036 lignocellulosic materials. *Waste and biomass valorization*, 9(5), 765-775.
- 1037 [2] Kunamneni, A. (2016). Cellulase in biomedical research. In *New and future*
1038 *developments in microbial biotechnology and bioengineering* (pp. 267-275).
1039 Elsevier.
- 1040 [3] Imran, M., Bano, S., Nazir, S., Javid, A., Asad, M. J., & Yaseen, A. (2019). Cellulases
1041 production and application of cellulases and accessory enzymes in pulp and paper
1042 industry: a review. *PSM Biological Research*, 4(1), 29-39.
- 1043 [4] Liu, W., Brennan, M. A., Serventi, L., & Brennan, C. S. (2017). Effect of cellulase,
1044 xylanase and α -amylase combinations on the rheological properties of Chinese
1045 steamed bread dough enriched in wheat bran. *Food chemistry*, 234, 93-102.
- 1046 [5] Huang, K., Won, W., Barnett, K. J., Brentzel, Z. J., Alonso, D. M., Huber, G. W., ... &
1047 Maravelias, C. T. (2018). Improving economics of lignocellulosic biofuels: An
1048 integrated strategy for coproducing 1, 5-pentanediol and ethanol. *Applied Energy*,
1049 213, 585-594.
- 1050 [6] Srivastava, N., Srivastava, M., Mishra, P. K., Gupta, V. K., Molina, G., Rodriguez-
1051 Couto, S., ... & Ramteke, P. W. (2018). Applications of fungal cellulases in biofuel
1052 production: advances and limitations. *Renewable and Sustainable Energy Reviews*,
1053 82, 2379-2386.

- 1054 [7] Tiwari, R., Nain, L., Labrou, N. E., & Shukla, P. (2018). Bioprospecting of functional
1055 cellulases from metagenome for second generation biofuel production: a review.
1056 *Critical reviews in microbiology*, 44(2), 244-257.
- 1057 [8] Adsul, M., Sandhu, S. K., Singhanian, R. R., Gupta, R., Puri, S. K., & Mathur, A. (2020).
1058 Designing a cellulolytic enzyme cocktail for the efficient and economical conversion
1059 of lignocellulosic biomass to biofuels. *Enzyme and microbial technology*, 133,
1060 109442.
- 1061 [9] Khoshnevisan, K., Vakhshiteh, F., Barkhi, M., Baharifar, H., Poor-Akbar, E., Zari, N.,
1062 ... & Bordbar, A. K. (2017). Immobilization of cellulase enzyme onto magnetic
1063 nanoparticles: Applications and recent advances. *Molecular Catalysis*, 442, 66-73.
- 1064 [10] Irfan, M., Ghazanfar, M., Rehman, A. U., & Siddique, A. (2019). Strategies to Reuse
1065 Cellulase: Immobilization of Enzymes (Part II). In *Approaches to Enhance Industrial
1066 Production of Fungal Cellulases* (pp. 137-151). Springer, Cham.
- 1067 [11] Goldhahn, C., Burgert, I., & Chanana, M. (2019). Nanoparticle-Mediated Enzyme
1068 Immobilization on Cellulose Fibers: Reusable Biocatalytic Systems for Cascade
1069 Reactions. *Advanced Materials Interfaces*, 6(19), 1900437.
- 1070 [12] Zhou, M., Ju, X., Zhou, Z., Yan, L., Chen, J., Yao, X., ... & Li, L. Z. (2019).
1071 Development of an Immobilized Cellulase System Based on Metal–Organic
1072 Frameworks for Improving Ionic Liquid Tolerance and In Situ Saccharification of
1073 Bagasse. *ACS Sustainable Chemistry & Engineering*, 7(23), 19185-19193.
- 1074 [13] Pandey, A. K., & Negi, S. (2020). Enhanced cellulase recovery in SSF from *Rhizopus*
1075 *oryzae* SN5 and immobilization for multi-batch saccharification of
1076 carboxymethylcellulose. *Biocatalysis and Agricultural Biotechnology*, 101656.
- 1077 [14] Juturu, V., & Wu, J. C. (2014). Microbial cellulases: engineering, production and
1078 applications. *Renewable and Sustainable Energy Reviews*, 33, 188-203.
- 1079 [15] Chapman, J., Ismail, A. E., & Dinu, C. Z. (2018). Industrial applications of enzymes:
1080 Recent advances, techniques, and outlooks. *Catalysts*, 8(6), 238.
- 1081 [16] Zhou, Z., Ju, X., Zhou, M., Xu, X., Fu, J., & Li, L. (2019). An enhanced ionic liquid-
1082 tolerant immobilized cellulase system via hydrogel microsphere for improving in situ
1083 saccharification of biomass. *Bioresource Technology*, 294, 122146.

- 1084 [17] Bilal, M., & Iqbal, H. M. (2019). Chemical, physical, and biological coordination: An
1085 interplay between materials and enzymes as potential platforms for immobilization.
1086 *Coordination Chemistry Reviews*, 388, 1-23.
- 1087 [18] Miletić, N., Nastasović, A., & Loos, K. (2012). Immobilization of biocatalysts for
1088 enzymatic polymerizations: possibilities, advantages, applications. *Bioresource*
1089 *Technology*, 115, 126-135.
- 1090 [19] Cacicedo, M. L., Manzo, R. M., Municoy, S., Bonazza, H. L., Islan, G. A., Desimone,
1091 M., ... & Castro, G. R. (2019). Immobilized enzymes and their applications. In
1092 *Advances in enzyme technology* (pp. 169-200). Elsevier.
- 1093 [20] Sillu, D., & Agnihotri, S. (2019). Cellulase Immobilization onto Magnetic Halloysite
1094 Nanotubes: Enhanced Enzyme Activity and Stability with High Cellulose
1095 Saccharification. *ACS Sustainable Chemistry & Engineering*, 8(2), 900-913.
- 1096 [21] Sui, Y., Cui, Y., Xia, G., Peng, X., Yuan, G., & Sun, G. (2019). A facile route to
1097 preparation of immobilized cellulase on polyurea microspheres for improving
1098 catalytic activity and stability. *Process Biochemistry*, 87, 73-82.
- 1099 [22] Wang, Y., Chen, D., Wang, G., Zhao, C., Ma, Y., & Yang, W. (2018). Immobilization
1100 of cellulase on styrene/maleic anhydride copolymer nanoparticles with improved
1101 stability against pH changes. *Chemical Engineering Journal*, 336, 152-159.
- 1102 [23] Lau, Y. S., & Yang, K. L. (2016). Entrapment of cross-linked cellulase colloids in
1103 alginate beads for hydrolysis of cellulose. *Colloids and Surfaces B: Biointerfaces*,
1104 145, 862-869.
- 1105 [24] Vaidyanath, S., Harish, B. S., Gayathri, G., Trilokesh, C., Uppuluri, K. B., &
1106 Anbazhagan, V. (2020). Maximizing the direct recovery and stabilization of
1107 cellulolytic enzymes from *Trichoderma harzanium* BPGF1 fermented broth using
1108 carboxymethyl inulin nanoparticles. *International Journal of Biological*
1109 *Macromolecules*.
- 1110 [25] Qamar, S. A., Asgher, M., & Bilal, M. (2020). Immobilization of Alkaline Protease
1111 From *Bacillus brevis* Using Ca-Alginate Entrapment Strategy for Improved Catalytic
1112 Stability, Silver Recovery, and Dehairing Potentialities. *Catalysis Letters*.
- 1113 [26] Xu, W., Sun, Z., Meng, H., Han, Y., Wu, J., Xu, J., ... & Zhang, X. (2018).
1114 Immobilization of cellulase proteins on zeolitic imidazolate framework (ZIF-

- 1115 8)/polyvinylidene fluoride hybrid membranes. *New Journal of Chemistry*, 42(21),
1116 17429-17438.
- 1117 [27] Mishra, A., & Sardar, M. (2015). Cellulase assisted synthesis of nano-silver and gold:
1118 application as immobilization matrix for biocatalysis. *International journal of*
1119 *biological macromolecules*, 77, 105-113.
- 1120 [28] Sánchez-Ramírez, J., Martínez-Hernández, J. L., Segura-Ceniceros, P., López, G.,
1121 Saade, H., Medina-Morales, M. A., ... & Ilyina, A. (2017). Cellulases immobilization
1122 on chitosan-coated magnetic nanoparticles: application for *Agave Atrovirens*
1123 lignocellulosic biomass hydrolysis. *Bioprocess and biosystems engineering*, 40(1),
1124 9-22.
- 1125 [29] Ladole, M. R., Mevada, J. S., & Pandit, A. B. (2017). Ultrasonic hyperactivation of
1126 cellulase immobilized on magnetic nanoparticles. *Bioresource technology*, 239,
1127 117-126.
- 1128 [30] Ashjari, M., Garmroodi, M., Ahrari, F., Yousefi, M., & Mohammadi, M. (2020). Soluble
1129 enzyme cross-linking via multi-component reactions: a new generation of cross-
1130 linked enzymes. *Chemical Communications*, 56(67), 9683-9686.
- 1131 [31] Wu, S. C., & Lia, Y. K. (2008). Application of bacterial cellulose pellets in enzyme
1132 immobilization. *Journal of Molecular Catalysis B: Enzymatic*, 54(3-4), 103-108.
- 1133 [32] Datta, S., Christena, L. R., & Rajaram, Y. R. S. (2013). Enzyme immobilization: an
1134 overview on techniques and support materials. *3 Biotech*, 3(1), 1-9.
- 1135 [33] Yuan, Y., Luan, X., Rana, X., Hassan, M. E., & Dou, D. (2016). Covalent
1136 immobilization of cellulase in application of biotransformation of ginsenoside Rb1.
1137 *Journal of Molecular Catalysis B: Enzymatic*, 133, S525-S532.
- 1138 [34] Jegannathan, K. R., Jun-Yee, L., Chan, E. S., & Ravindra, P. (2010). Production of
1139 biodiesel from palm oil using liquid core lipase encapsulated in κ -carrageenan. *Fuel*,
1140 89(9), 2272-2277.
- 1141 [35] Zhao, X., Qi, F., Yuan, C., Du, W., & Liu, D. (2015). Lipase-catalyzed process for
1142 biodiesel production: Enzyme immobilization, process simulation and optimization.
1143 *Renewable and Sustainable Energy Reviews*, 44, 182-197.

- 1144 [36] Chang, R. H. Y., Jang, J., & Wu, K. C. W. (2011). Cellulase immobilized mesoporous
1145 silica nano catalysts for efficient cellulose-to-glucose conversion. *Green Chemistry*,
1146 13(10), 2844-2850.
- 1147 [37] Ur Rehman, A., Kovacs, Z., Quitmann, H., Ebrahimi, M., & Czermak, P. (2016).
1148 Enzymatic production of fructooligosaccharides from inexpensive and abundant
1149 substrates using a membrane reactor system. *Separation Science and Technology*,
1150 51(9), 1537-1545.
- 1151 [38] Fraser, J. E., & Bickerstaff, G. F. (1997). Entrapment in calcium alginate. In
1152 *Immobilization of enzymes and cells* (pp. 61-66). Humana Press.
- 1153 [39] Blandino, A., Macias, M., & Cantero, D. (1999). Formation of calcium alginate gel
1154 capsules: influence of sodium alginate and CaCl₂ concentration on gelation kinetics.
1155 *Journal of bioscience and bioengineering*, 88(6), 686-689.
- 1156 [40] Simó, G., Fernández-Fernández, E., Vila-Crespo, J., Ruipérez, V., & Rodríguez-
1157 Nogales, J. M. (2017). Research progress in coating techniques of alginate gel
1158 polymer for cell encapsulation. *Carbohydrate polymers*, 170, 1-14.
- 1159 [41] Andriani, D., Sunwoo, C., Ryu, H. W., Prasetya, B., & Park, D. H. (2012).
1160 Immobilization of cellulase from newly isolated strain *Bacillus subtilis* TD6 using
1161 calcium alginate as a support material. *Bioprocess and biosystems engineering*,
1162 35(1-2), 29-33.
- 1163 [42] Imran, M., Hussain, A., Anwar, Z., Zeeshan, N., Yaseen, A., Akmal, M., & Idris, M.
1164 (2020). Immobilization of Fungal Cellulase on Calcium Alginate and Xerogel Matrix.
1165 *Waste and Biomass Valorization*, 11(4), 1229-1237.
- 1166 [43] Guo, R., Zheng, X., Wang, Y., Yang, Y., Ma, Y., Zou, D., & Liu, Y. (2021).
1167 Optimization of Cellulase Immobilization with Sodium Alginate-Polyethylene for
1168 Enhancement of Enzymatic Hydrolysis of Microcrystalline Cellulose Using
1169 Response Surface Methodology. *Applied Biochemistry and Biotechnology*, 1-18.
- 1170 [44] Viet, T. Q., Minh, N. P., & Dao, D. T. A. (2013). Immobilization of cellulase enzyme
1171 in calcium alginate gel and its immobilized stability. *American Journal of Research*
1172 *Communication*, 1(12), 254-267.

- 1173 [45] Sankarraaj, N., & Nallathambi, G. (2015). Immobilization and characterization of
1174 cellulase on concanavalin A (Con A)-layered calcium alginate beads. *Biocatalysis
1175 and Biotransformation*, 33(2), 81-88.
- 1176 [46] Abdel-Sater, M., Hussein, N., Fetyan, N., & Gad, S. (2019). Immobilization of
1177 Cellulases Produced by *Penicillium brevicompactum* AUMC 10987, using Cross-
1178 Linkage, Chitosan-Coating and Encapsulation. *Catrina: The International Journal of
1179 Environmental Sciences*, 18(1), 139-149.
- 1180 [47] Jahangeer, M., Qamar, S. A., Mahmood, Z., & Asgher, M. (2019). Applications and
1181 perspectives of chitosan as functional biopolymer; an extended review. *Life Science
1182 Journal of Pakistan*, 1(2), 33-40.
- 1183 [48] Eskandari, L., Andalib, F., Fakhri, A., Jabarabadi, M. K., Pham, B., & Gupta, V. K.
1184 (2020). Facile colorimetric detection of Hg (II), photocatalytic and antibacterial
1185 efficiency based on silver-manganese disulfide/polyvinyl alcohol-chitosan
1186 nanocomposites. *International Journal of Biological Macromolecules*, 164, 4138-
1187 4145.
- 1188 [49] Abd El-Ghaffar, M. A., & Hashem, M. S. (2010). Chitosan and its amino acids
1189 condensation adducts as reactive natural polymer supports for cellulase
1190 immobilization. *Carbohydrate polymers*, 81(3), 507-516.
- 1191 [50] Miao, X., Pi, L., Fang, L., Wu, R., & Xiong, C. (2016). Application and characterization
1192 of magnetic chitosan microspheres for enhanced immobilization of cellulase.
1193 *Biocatalysis and Biotransformation*, 34(6), 272-282.
- 1194 [51] Díaz-Hernández, A., Gracida, J., García-Almendárez, B. E., Regalado, C., Núñez,
1195 R., & Amaro-Reyes, A. (2018). Characterization of magnetic nanoparticles coated
1196 with chitosan: A potential approach for enzyme immobilization. *Journal of
1197 Nanomaterials*, 2018.
- 1198 [52] Mo, H., Qiu, J., Yang, C., Zang, L., Sakai, E., & Chen, J. (2020). Porous
1199 biochar/chitosan composites for high performance cellulase immobilization by
1200 glutaraldehyde. *Enzyme and Microbial Technology*, 109561.
- 1201 [53] Mo, H., & Qiu, J. (2020a). Preparation of Chitosan/Magnetic Porous Biochar as
1202 Support for Cellulase Immobilization by Using Glutaraldehyde. *Polymers*, 12(11),
1203 2672.

- 1204 [54] Yu, Y., Yuan, J., Wang, Q., Fan, X., & Wang, P. (2012). Covalent immobilization of
1205 cellulases onto a water-soluble–insoluble reversible polymer. *Applied biochemistry
1206 and biotechnology*, 166(6), 1433-1441.
- 1207 [55] Ince, A., Bayramoglu, G., Karagoz, B., Altintas, B., Bicak, N., & Arica, M. Y. (2012).
1208 A method for fabrication of polyaniline coated polymer microspheres and its
1209 application for cellulase immobilization. *Chemical engineering journal*, 189, 404-
1210 412.
- 1211 [56] Romo-Sánchez, S., Camacho, C., Ramirez, H. L., & Arévalo-Villena, M. (2014).
1212 Immobilization of commercial cellulase and xylanase by different methods using two
1213 polymeric supports. *Advances in Bioscience and Biotechnology*, 5(06), 517.
- 1214 [57] Lu, L., Zhang, L., Yuan, L., Zhu, T., Chen, W., Wang, G., & Wang, Q. (2019). Artificial
1215 Cellulosome Complex from the Self-Assembly of Ni-NTA-Functionalized Polymeric
1216 Micelles and Cellulases. *ChemBioChem*, 20(11), 1394-1399.
- 1217 [58] Ding, Z., Zheng, X., Li, S., & Cao, X. (2016). Immobilization of cellulase onto a
1218 recyclable thermo-responsive polymer as bioconjugate. *Journal of Molecular
1219 Catalysis B: Enzymatic*, 128, 39-45.
- 1220 [59] Tąta, A., Sokołowska, K., Świder, J., Konieczna-Molenda, A., Proniewicz, E., &
1221 Witek, E. (2015). Study of cellulolytic enzyme immobilization on copolymers of N-
1222 vinylformamide. *Spectrochimica Acta Part A: Molecular and Biomolecular
1223 Spectroscopy*, 149, 494-504.
- 1224 [60] Wang, Y., Qi, Y., Chen, C., Zhao, C., Ma, Y., & Yang, W. (2019). Layered Co-
1225 Immobilization of β -Glucosidase and Cellulase on Polymer Film by Visible-Light-
1226 Induced Graft Polymerization. *ACS Applied Materials & Interfaces*, 11(47), 44913-
1227 44921.
- 1228 [61] Lei, C., Shin, Y., Liu, J., & Ackerman, E. J. (2002). Entrapping enzyme in a
1229 functionalized nanoporous support. *Journal of the American Chemical Society*,
1230 124(38), 11242-11243.
- 1231 [62] Han, Y. J., Stucky, G. D., & Butler, A. (1999). Mesoporous silicate sequestration and
1232 release of proteins. *Journal of the American Chemical Society*, 121(42), 9897-9898.
- 1233 [63] Poorakbar, E., Shafiee, A., Saboury, A. A., Rad, B. L., Khoshnevisan, K., Ma'mani,
1234 L., ... & Hosseini, M. (2018). Synthesis of magnetic gold mesoporous silica

1235 nanoparticles core shell for cellulase enzyme immobilization: Improvement of
1236 enzymatic activity and thermal stability. *Process biochemistry*, 71, 92-100.

1237 [64] Dai, H., Ou, S., Liu, Z., & Huang, H. (2017). Pineapple peel carboxymethyl
1238 cellulose/polyvinyl alcohol/mesoporous silica SBA-15 hydrogel composites for
1239 papain immobilization. *Carbohydrate polymers*, 169, 504-514.

1240 [65] Xiang, X., Ding, S., Suo, H., Xu, C., Gao, Z., & Hu, Y. (2018). Fabrication of chitosan-
1241 mesoporous silica SBA-15 nanocomposites via functional ionic liquid as the bridging
1242 agent for PPL immobilization. *Carbohydrate polymers*, 182, 245-253.

1243 [66] Takimoto, A., Shiomi, T., Ino, K., Tsunoda, T., Kawai, A., Mizukami, F., & Sakaguchi,
1244 K. (2008). Encapsulation of cellulase with mesoporous silica (SBA-15). *Microporous
1245 and Mesoporous Materials*, 116(1-3), 601-606.

1246 [67] Hartono, S. B., Qiao, S. Z., Liu, J., Jack, K., Ladewig, B. P., Hao, Z., & Lu, G. Q. M.
1247 (2010). Functionalized mesoporous silica with very large pores for cellulase
1248 immobilization. *The Journal of Physical Chemistry C*, 114(18), 8353-8362.

1249 [68] Harmoko, C., Sucipto, K. I., Retnoningtyas, E. S., & Hartono, S. B. (2016). Vinyl
1250 functionalized cubic mesoporous silica nanoparticles as supporting material to
1251 enhance cellulase enzyme stability. *ARNP J Eng Appl Sci*, 11, 2981-2992.

1252 [69] Chang, K. L., Thitikorn-Amorn, J., Chen, S. H., Hsieh, J. F., Ratanakhanokchai, K.,
1253 Huang, P. J., ... & Chen, S. T. (2011). Improving the remaining activity of
1254 lignocellulolytic enzymes by membrane entrapment. *Bioresource technology*,
1255 102(2), 519-523.

1256 [70] Dadi, A. P., Varanasi, S., & Schall, C. A. (2006). Enhancement of cellulose
1257 saccharification kinetics using an ionic liquid pretreatment step. *Biotechnology and
1258 bioengineering*, 95(5), 904-910.

1259 [71] Kannan, K., & Jasra, R. V. (2011). Improved catalytic hydrolysis of carboxy methyl
1260 cellulose using cellulase immobilized on functionalized meso cellular foam. *Journal
1261 of Porous Materials*, 18(4), 409-416.

1262 [72] Yin, H., Su, Z. L., Shao, H., Cai, J., Wang, X., & Yin, H. (2013). Immobilization of
1263 cellulase on modified mesoporous silica shows improved thermal stability and
1264 reusability. *African Journal of Microbiology Research*, 7(25), 3248-3253.

- 1265 [73] Zhang, D., Hegab, H. E., Lvov, Y., Snow, L. D., & Palmer, J. (2016). Immobilization
1266 of cellulase on a silica gel substrate modified using a 3-APTES self-assembled
1267 monolayer. *SpringerPlus*, 5(1), 1-20.
- 1268 [74] Ungurean, M., Paul, C., & Peter, F. (2013). Cellulase immobilized by sol-gel
1269 entrapment for efficient hydrolysis of cellulose. *Bioprocess and biosystems
1270 engineering*, 36(10), 1327-1338.
- 1271 [75] Chen, B., Qiu, J., Mo, H., Yu, Y., Ito, K., Sakai, E., & Feng, H. (2017). Synthesis of
1272 mesoporous silica with different pore sizes for cellulase immobilization: pure
1273 physical adsorption. *New Journal of Chemistry*, 41(17), 9338-9345.
- 1274 [76] Pavlidis, I. V., Vorhaben, T., Gournis, D., Papadopoulos, G. K., Bornscheuer, U. T.,
1275 & Stamatis, H. (2012). Regulation of catalytic behaviour of hydrolases through
1276 interactions with functionalized carbon-based nanomaterials. *Journal of
1277 Nanoparticle Research*, 14(5), 842.
- 1278 [77] Pavlidis, I. V., Patila, M., Bornscheuer, U. T., Gournis, D., & Stamatis, H. (2014).
1279 Graphene-based nanobiocatalytic systems: recent advances and future prospects.
1280 *Trends in biotechnology*, 32(6), 312-320.
- 1281 [78] Schwaminger, S. P., Fraga-García, P., Selbach, F., Hein, F. G., Fuß, E. C., Surya,
1282 R., ... & Berensmeier, S. (2017). Bio-nano interactions: Cellulase on iron oxide
1283 nanoparticle surfaces. *Adsorption*, 23(2-3), 281-292.
- 1284 [79] Patila, M., Pavlidis, I. V., Kouloumpis, A., Dimos, K., Spyrou, K., Katapodis, P., ... &
1285 Stamatis, H. (2016). Graphene oxide derivatives with variable alkyl chain length and
1286 terminal functional groups as supports for stabilization of cytochrome c. *International
1287 journal of biological macromolecules*, 84, 227-235.
- 1288 [80] Khoshnevisan, K., Bordbar, A. K., Zare, D., Davoodi, D., Noruzi, M., Barkhi, M., &
1289 Tabatabaei, M. (2011). Immobilization of cellulase enzyme on superparamagnetic
1290 nanoparticles and determination of its activity and stability. *Chemical engineering
1291 journal*, 171(2), 669-673.
- 1292 [81] Abraham, R. E., Verma, M. L., Barrow, C. J., & Puri, M. (2014). Suitability of magnetic
1293 nanoparticle immobilised cellulases in enhancing enzymatic saccharification of
1294 pretreated hemp biomass. *Biotechnology for biofuels*, 7(1), 90.

- 1295 [82] Qi, H., Duan, H., Wang, X., Meng, X., Yin, X., & Ma, L. (2015). Preparation of
1296 magnetic porous terpolymer and its application in cellulase immobilization. *Polymer*
1297 *Engineering & Science*, 55(5), 1039-1045.
- 1298 [83] Abbaszadeh, M., & Hejazi, P. (2019). Metal affinity immobilization of cellulase on
1299 Fe₃O₄ nanoparticles with copper as ligand for biocatalytic applications. *Food*
1300 *chemistry*, 290, 47-55.
- 1301 [84] Mo, H., Qiu, J., Yang, C., Zang, L., & Sakai, E. (2020b). Preparation and
1302 characterization of magnetic polyporous biochar for cellulase immobilization by
1303 physical adsorption. *Cellulose*, 27(9), 4963-4973.
- 1304 [85] Paz-Cedeno, F. R., Carceller, J. M., Iborra, S., Donato, R. K., Godoy, A. P., de Paula,
1305 A. V., ... & Masarin, F. (2021). Magnetic graphene oxide as a platform for the
1306 immobilization of cellulases and xylanases: Ultrastructural characterization and
1307 assessment of lignocellulosic biomass hydrolysis. *Renewable Energy*, 164, 491-
1308 501.
- 1309 [86] Bilal, M., Zhao, Y., Noreen, S., Shah, S. Z. H., Bharagava, R. N., & Iqbal, H. M.
1310 (2019). Modifying bio-catalytic properties of enzymes for efficient biocatalysis: A
1311 review from immobilization strategies viewpoint. *Biocatalysis and Biotransformation*,
1312 37(3), 159-182.
- 1313 [87] Cao, L., van Rantwijk, F., & Sheldon, R. A. (2000). Cross-linked enzyme aggregates:
1314 a simple and effective method for the immobilization of penicillin acylase. *Organic*
1315 *letters*, 2(10), 1361-1364.
- 1316 [88] Asgher, M., Bashir, F., & Iqbal, H. M. (2018). Protease-based cross-linked enzyme
1317 aggregates with improved catalytic stability, silver removal, and dehairing potentials.
1318 *International journal of biological macromolecules*, 118, 1247-1256.
- 1319 [89] Bashir, F., Asgher, M., Hussain, F., & Randhawa, M. A. (2018). Development and
1320 characterization of cross-linked enzyme aggregates of thermotolerant alkaline
1321 protease from *Bacillus licheniformis*. *International journal of biological*
1322 *macromolecules*, 113, 944-951.
- 1323 [90] Wilson, L., Illanes, A., Pessela, B. C., Abian, O., Fernández-Lafuente, R., & Guisán,
1324 J. M. (2004). Encapsulation of crosslinked penicillin G acylase aggregates in

- 1325 lentikats: evaluation of a novel biocatalyst in organic media. *Biotechnology and*
1326 *bioengineering*, 86(5), 558-562.
- 1327 [91] Kim, M. I., Kim, J., Lee, J., Jia, H., Na, H. B., Youn, J. K., ... & Chang, H. N. (2007).
1328 Crosslinked enzyme aggregates in hierarchically-ordered mesoporous silica: A
1329 simple and effective method for enzyme stabilization. *Biotechnology and*
1330 *bioengineering*, 96(2), 210-218.
- 1331 [92] Periyasamy, K., Santhalembi, L., Mortha, G., Aurousseau, M., & Subramanian, S.
1332 (2016). Carrier-free co-immobilization of xylanase, cellulase and β -1, 3-glucanase
1333 as combined cross-linked enzyme aggregates (combi-CLEAs) for one-pot
1334 saccharification of sugarcane bagasse. *RSC advances*, 6(39), 32849-32857.
- 1335 [93] Perzon, A., Dicko, C., Çobanoğlu, Ö., Yükselen, O., Eryilmaz, J., & Dey, E. S. (2017).
1336 Cellulase cross-linked enzyme aggregates (CLEA) activities can be modulated and
1337 enhanced by precipitant selection. *Journal of Chemical Technology &*
1338 *Biotechnology*, 92(7), 1645-1649.
- 1339 [94] Podrepšek, G. H., Knez, Ž., & Leitgeb, M. (2019). Activation of cellulase cross-linked
1340 enzyme aggregates (CLEAs) in scCO₂. *The Journal of Supercritical Fluids*, 154,
1341 104629.
- 1342 [95] Asgher, M., Afzal, M., Qamar, S. A., & Khalid, N. (2020b). Optimization of
1343 biosurfactant production from chemically mutated strain of *Bacillus subtilis* using
1344 waste automobile oil as low-cost substrate. *Environmental Sustainability*, 3(4), 405-
1345 413.
- 1346 [96] Asgher, M., Arshad, S., Qamar, S. A., & Khalid, N. (2020c). Improved biosurfactant
1347 production from *Aspergillus niger* through chemical mutagenesis: characterization
1348 and RSM optimization. *SN Applied Sciences*, 2(5), 1-11.
- 1349 [97] Qamar, S. A., Asgher, M., & Bilal, M. (2021). Sustainable Production, Optimization,
1350 and Partial Characterization of Exopolysaccharides by *Macrococcus brunensis*.
1351 *Waste and Biomass Valorization*, 1-13.
- 1352 [98] Asgher, M., Qamar, S. A., Bilal, M., & Iqbal, H. M. (2020d). Bio-based active food
1353 packaging materials: Sustainable alternative to conventional petrochemical-based
1354 packaging materials. *Food Research International*, 109625.

- 1355 [99] Asgher, M., Rani, A., Khalid, N., Qamar, S. A., & Bilal, M. (2021). Bioconversion of
1356 sugarcane molasses waste to high-value exopolysaccharides by engineered
1357 *Bacillus licheniformis*. *Case Studies in Chemical and Environmental Engineering*,
1358 100084.
- 1359 [100] Asgher, M., Urooj, Y., Qamar, S. A., & Khalid, N. (2020a). Improved
1360 exopolysaccharide production from *Bacillus licheniformis* MS3: optimization and
1361 structural/functional characterization. *International journal of biological*
1362 *macromolecules*, 151, 984-992.
- 1363 [101] Jia, J., Zhang, W., Yang, Z., Yang, X., Wang, N., & Yu, X. (2017). Novel magnetic
1364 cross-linked cellulase aggregates with a potential application in lignocellulosic
1365 biomass bioconversion. *Molecules*, 22(2), 269.
- 1366 [102] Jafari Khorshidi, K., Lenjannezhadian, H., Jamalana, M., & Zeinali, M. (2016).
1367 Preparation and characterization of nanomagnetic cross-linked cellulase
1368 aggregates for cellulose bioconversion. *Journal of Chemical Technology &*
1369 *Biotechnology*, 91(2), 539-546.
- 1370 [103] Li, B., Dong, S. L., Xie, X. L., Xu, Z. B., & Li, L. (2012). Preparation and properties
1371 of cross-linked enzyme aggregates of cellulase. In *Advanced Materials Research*
1372 (Vol. 581, pp. 257-260). Trans Tech Publications Ltd.
- 1373 [104] Ashraf, M. A., Li, C., Zhang, D., Zhao, L., & Fakhri, A. (2021). Fabrication of silver
1374 phosphate-ilmenite nanocomposites supported on glycol chitosan for visible light-
1375 driven degradation, and antimicrobial activities. *International Journal of Biological*
1376 *Macromolecules*, 169, 436-442.
- 1377 [105] Ray, C., & Pal, T. (2017). Retracted Article: Recent advances of metal–metal oxide
1378 nanocomposites and their tailored nanostructures in numerous catalytic
1379 applications. *Journal of Materials Chemistry A*, 5(20), 9465-9487.
- 1380 [106] Yang, Y., Ashraf, M. A., Fakhri, A., Gupta, V. K., & Zhang, D. (2021). Facile
1381 synthesis of gold-silver/copper sulfide nanoparticles for the selective/sensitive
1382 detection of chromium, photochemical and bactericidal application. *Spectrochimica*
1383 *Acta Part A: Molecular and Biomolecular Spectroscopy*, 249, 119324.
- 1384 [107] Huang, M., Zhang, R., Yang, Z., Chen, J., Deng, J., Fakhri, A., & Gupta, V. K.
1385 (2020). Synthesis of Co₃S₄-SnO₂/polyvinylpyrrolidone-cellulose heterojunction as

- 1386 highly performance catalyst for photocatalytic and antimicrobial properties under
1387 ultra-violet irradiation. *International Journal of Biological Macromolecules*, 162, 220-
1388 228.
- 1389 [108] Cai, Y., Yang, F., Wu, L., Shu, Y., Qu, G., Fakhri, A., & Gupta, V. K. (2021).
1390 Hydrothermal-ultrasonic synthesis of CuO nanorods and CuWO₄ nanoparticles for
1391 catalytic reduction, photocatalysis activity, and antibacterial properties. *Materials*
1392 *Chemistry and Physics*, 258, 123919.
- 1393 [109] Jordan, J., Kumar, C. S., & Theegala, C. (2011). Preparation and characterization
1394 of cellulase-bound magnetite nanoparticles. *Journal of Molecular Catalysis B:*
1395 *Enzymatic*, 68(2), 139-146.
- 1396 [110] Zhang, J., Ding, E., Xu, S., Li, Z., Fakhri, A., & Gupta, V. K. (2020). Production of
1397 metal oxides nanoparticles based on poly-alanine/chitosan/reduced graphene oxide
1398 for photocatalysis degradation, anti-pathogenic bacterial and antioxidant studies.
1399 *International Journal of Biological Macromolecules*, 164, 1584-1591.
- 1400 [111] Xu, J., Huo, S., Yuan, Z., Zhang, Y., Xu, H., Guo, Y., ... & Zhuang, X. (2011).
1401 Characterization of direct cellulase immobilization with superparamagnetic
1402 nanoparticles. *Biocatalysis and biotransformation*, 29(2-3), 71-76.
- 1403 [112] Han, J., Wang, L., Wang, Y., Dong, J., Tang, X., Ni, L., & Wang, L. (2018).
1404 Preparation and characterization of Fe₃O₄-NH₂@ 4-arm-PEG-NH₂, a novel
1405 magnetic four-arm polymer-nanoparticle composite for cellulase immobilization.
1406 *Biochemical Engineering Journal*, 130, 90-98.
- 1407 [113] Mubarak, N. M., Wong, J. R., Tan, K. W., Sahu, J. N., Abdullah, E. C., Jayakumar,
1408 N. S., & Ganesan, P. (2014). Immobilization of cellulase enzyme on functionalized
1409 multiwall carbon nanotubes. *Journal of Molecular Catalysis B: Enzymatic*, 107, 124-
1410 131.
- 1411 [114] Ahmad, R., & Khare, S. K. (2018). Immobilization of *Aspergillus niger* cellulase on
1412 multiwall carbon nanotubes for cellulose hydrolysis. *Bioresource technology*, 252,
1413 72-75.
- 1414 [115] Ma'an, F. A., Alam, M. Z., & Mohammed, R. (2012). Statistical modelling
1415 optimisation of cellulase enzyme immobilisation on functionalised multi-walled

- 1416 carbon nanotubes for empty fruit bunches degradation. Australian Journal of Basic
1417 and Applied Sciences, 6(1), 30-38.
- 1418 [116] Li, L. J., Xia, W. J., Ma, G. P., Chen, Y. L., & Ma, Y. Y. (2019). A study on the
1419 enzymatic properties and reuse of cellulase immobilized with carbon nanotubes and
1420 sodium alginate. *Amb Express*, 9(1), 1-8.
- 1421 [117] Azahari, N. Y. H., Sandrakesaran, N., Connie, C. C. G., & Balakrishnan, K. (2020,
1422 May). Immobilization of Cellulase from *Trichoderma Reesei* on Multiwall Carbon
1423 Nanotubes (MWCNTs). In *IOP Conference Series: Materials Science and
1424 Engineering* (Vol. 864, No. 1, p. 012171). IOP Publishing.
- 1425 [118] Gokhale, A. A., Lu, J., & Lee, I. (2013). Immobilization of cellulase on magneto
1426 responsive graphene nano-supports. *Journal of Molecular Catalysis B: Enzymatic*,
1427 90, 76-86.
- 1428 [119] Gao, J., Lu, C. L., Wang, Y., Wang, S. S., Shen, J. J., Zhang, J. X., & Zhang, Y. W.
1429 (2018). Rapid immobilization of cellulase onto graphene oxide with a hydrophobic
1430 spacer. *Catalysts*, 8(5), 180.
- 1431 [120] Zhang, H., Hua, S. F., & Zhang, L. (2020). Co-immobilization of cellulase and
1432 glucose oxidase on graphene oxide by covalent bonds: a biocatalytic system for
1433 one-pot conversion of gluconic acid from carboxymethyl cellulose. *Journal of
1434 Chemical Technology & Biotechnology*, 95(4), 1116-1125.
- 1435 [121] Tran, T. D., & Kim, M. I. (2018). Organic-inorganic hybrid nanoflowers as potent
1436 materials for biosensing and biocatalytic applications. *BioChip Journal*, 12(4), 268-
1437 279.
- 1438 [122] Bilal, M., Qamar, S. A., Ashraf, S. S., Rodríguez-Couto, S., & Iqbal, H. M. (2021).
1439 Robust nanocarriers to engineer nanobiocatalysts for bioprocessing applications.
1440 *Advances in Colloid and Interface Science*, 102438.
- 1441 [123] Batule, B. S., Park, K. S., Kim, M. I., & Park, H. G. (2015). Ultrafast sonochemical
1442 synthesis of protein-inorganic nanoflowers. *International journal of nanomedicine*,
1443 10(Spec Iss), 137.
- 1444 [124] Wang, L. B., Wang, Y. C., He, R., Zhuang, A., Wang, X., Zeng, J., & Hou, J. G.
1445 (2013). A new nanobiocatalytic system based on allosteric effect with dramatically

1446 enhanced enzymatic performance. *Journal of the American Chemical Society*,
1447 135(4), 1272-1275.

1448 [125] Zdarta, J., Jędrzak, A., Kłapiszewski, Ł., & Jesionowski, T. (2017). Immobilization
1449 of cellulase on a functional inorganic–organic hybrid support: stability and kinetic
1450 study. *Catalysts*, 7(12), 374.

1451 [126] Dragomirescu, M., Vintila, T., & Preda, G. (2011). Immobilized Microbial Cellulases
1452 in Organic-Inorganic Hybrid Materials. *Scientific Papers Animal Science and
1453 Biotechnologies*, 44(1), 380-383.

1454 [127] Cipolatti, E. P., Valerio, A., Henriques, R. O., Moritz, D. E., Ninow, J. L., Freire, D.
1455 M., ... & de Oliveira, D. (2016). Nanomaterials for biocatalyst immobilization–state
1456 of the art and future trends. *RSC advances*, 6(106), 104675-104692.

1457 [128] Bilal, M., Asgher, M., Shah, S. Z. H., & Iqbal, H. M. (2019). Engineering enzyme-
1458 coupled hybrid nanoflowers: The quest for optimum performance to meet
1459 biocatalytic challenges and opportunities. *International journal of biological
1460 macromolecules*, 135, 677-690.

1461 [129] Cen, S., Lv, X., Jiang, Y., Fakhri, A., & Gupta, V. K. (2020). Synthesis and structure
1462 of iron–copper/hollow magnetic/metal–organic framework/coordination sites in a
1463 heterogeneous catalyst for a Fenton-based reaction. *Catalysis Science &
1464 Technology*, 10(19), 6687-6693.

1465 [130] Liang, S., Wu, X. L., Xiong, J., Zong, M. H., & Lou, W. Y. (2020). Metal-organic
1466 frameworks as novel matrices for efficient enzyme immobilization: an update review.
1467 *Coordination Chemistry Reviews*, 406, 213149.

1468 [131] Wen, J., Liu, X., Liu, L., Ma, X., Fakhri, A., & Gupta, V. K. (2021). Bimetal cobalt-
1469 Iron based organic frameworks with coordinated sites as synergistic catalyst for
1470 fenton catalysis study and antibacterial efficiency. *Colloids and Surfaces A:
1471 Physicochemical and Engineering Aspects*, 610, 125683.

1472 [132] Ahmed, I. N., Yang, X. L., Dubale, A. A., Li, R. F., Ma, Y. M., Wang, L. M., ... & Xie,
1473 M. H. (2018). Hydrolysis of cellulose using cellulase physically immobilized on highly
1474 stable zirconium-based metal-organic frameworks. *Bioresource technology*, 270,
1475 377-382.

- 1476 [133] Qi, B., Luo, J., & Wan, Y. (2018). Immobilization of cellulase on a core-shell
1477 structured metal-organic framework composites: Better inhibitors tolerance and
1478 easier recycling. *Bioresource technology*, 268, 577-582.
- 1479 [134] De Corato, U., De Bari, I., Viola, E., & Pugliese, M. (2018). Assessing the main
1480 opportunities of integrated biorefining from agro-bioenergy co/by-products and
1481 agroindustrial residues into high-value added products associated to some
1482 emerging markets: A review. *Renewable and Sustainable Energy Reviews*, 88, 326-
1483 346.
- 1484 [135] Periyasamy, K., Santhalembi, L., Mortha, G., Aurousseau, M., Boyer, A., &
1485 Subramanian, S. (2018). Bioconversion of lignocellulosic biomass to fermentable
1486 sugars by immobilized magnetic cellulolytic enzyme cocktails. *Langmuir*, 34(22),
1487 6546-6555.
- 1488 [136] Hu, J., Arantes, V., Pribowo, A., Gourlay, K., & Saddler, J. N. (2014). Substrate
1489 factors that influence the synergistic interaction of AA9 and cellulases during the
1490 enzymatic hydrolysis of biomass. *Energy & Environmental Science*, 7(7), 2308-
1491 2315.
- 1492 [137] Rahman, S. A., Masjuki, H. H., Kalam, M. A., Abedin, M. J., Sanjid, A., & Sajjad, H.
1493 (2013). Production of palm and Calophyllum inophyllum based biodiesel and
1494 investigation of blend performance and exhaust emission in an unmodified diesel
1495 engine at high idling conditions. *Energy Conversion and Management*, 76, 362-367.
- 1496 [138] Tian, S. Q., Zhao, R. Y., & Chen, Z. C. (2018). Review of the pretreatment and
1497 bioconversion of lignocellulosic biomass from wheat straw materials. *Renewable
1498 and Sustainable Energy Reviews*, 91, 483-489.
- 1499 [139] Seidl, P. R., & Goulart, A. K. (2016). Pretreatment processes for lignocellulosic
1500 biomass conversion to biofuels and bioproducts. *Current Opinion in Green and
1501 Sustainable Chemistry*, 2, 48-53.
- 1502 [140] Vaishnav N, Singh N, Adsul M, Dixit P (2018) Penicillium: the next emerging
1503 champion for cellulase. *Bioresour Technol Rep* 2:131–140.
- 1504 [141] Jadhav AR, Girdhe AV, More SM, More SB, Khan S (2013) Cellulase production by
1505 utilizing agricultural wastes. *Res J Agric For Sci* 1(7):6–9.

- 1506 [142] Manfredi AP, Ballesteros I, Sáez F, Perotti NI, Martínez MA, Negro MJ (2018)
1507 Integral process assessment of sugarcane agricultural crop residues conversion to
1508 ethanol. *Bioresour Technol* 260:241–247.
- 1509 [143] Zacharia, K. M. B., Yadav, S., Machhirake, N. P., Kim, S. H., Lee, B. D., Jeong, H.,
1510 ... & Kumar, R. (2020). Bio-hydrogen and bio-methane potential analysis for
1511 production of bio-hythane using various agricultural residues. *Bioresource*
1512 *Technology*, 123297.
- 1513 [144] Ingle, A. P., Rathod, J., Pandit, R., da Silva, S. S., & Rai, M. (2017). Comparative
1514 evaluation of free and immobilized cellulase for enzymatic hydrolysis of
1515 lignocellulosic biomass for sustainable bioethanol production. *Cellulose*, 24(12),
1516 5529-5540.
- 1517 [145] Thomas, L., Ram, H., Kumar, A., & Singh, V. P. (2013). Industrial and
1518 biotechnological potential of microbial cellulases. *Journal of Plant Development*
1519 *Sciences Vol, 5(3), 237-247.*
- 1520 [146] Sharada, R., Venkateswarlu, G., Venkateswar, S., & Rao, M. A. (2014).
1521 APPLICATIONS OF CELLULASES-REVIEW. *International Journal of*
1522 *Pharmaceutical, Chemical & Biological Sciences*, 4(2).
- 1523 [147] Singh, A., Kuhad, R. C., & Ward, O. P. (2007). Industrial application of microbial
1524 cellulases. *Lignocellulose biotechnology: Future prospects*, 345-358.
- 1525 [148] Willberg-Keyriläinen, P., Ropponen, J., Lahtinen, M., & Pere, J. (2019). Improved
1526 reactivity and derivatization of cellulose after pre-hydrolysis with commercial
1527 enzymes. *BioResources*, 14(1), 561-574.
- 1528 [149] Kuhad, R. C., Gupta, R., & Singh, A. (2011). Microbial cellulases and their industrial
1529 applications. *Enzyme research*, 2011.
- 1530 [150] Yang, M., Lu, F., Zhou, T., Zhao, J., Ding, C., Fakhri, A., & Gupta, V. K. (2020).
1531 Biosynthesis of nano bimetallic Ag/Pt alloy from *Crocus sativus* L. extract: biological
1532 efficacy and catalytic activity. *Journal of Photochemistry and Photobiology B:*
1533 *Biology*, 212, 112025.
- 1534 [151] Kuhad, R. C., Mehta, G., Gupta, R., & Sharma, K. K. (2010). Fed batch enzymatic
1535 saccharification of newspaper cellulosics improves the sugar content in the

1536 hydrolysates and eventually the ethanol fermentation by *Saccharomyces*
1537 *cerevisiae*. *Biomass and Bioenergy*, 34(8), 1189-1194.

1538 [152] Liu, R. H., Dai, S. A., Chang, F. J., Cheng, W. T., & Shih, Y. F. (2010). Highly
1539 efficient PET film-assisted adsorption process for the de-inking of xerographic
1540 wastepaper. *Journal of the Taiwan institute of Chemical Engineers*, 41(3), 344-351.

1541 [153] Yassin, M. A., Gad, A. A. M., Ghanem, A. F., & Rehim, M. H. A. (2019). Green
1542 synthesis of cellulose nanofibers using immobilized cellulase. *Carbohydrate*
1543 *polymers*, 205, 255-260.

1544 [154] Soares, J. F., Dal Prá, V., Kempka, A. P., Prestes, R. C., Tres, M. V., Kuhn, R. C.,
1545 & Mazutti, M. A. (2016). Cellulases for food applications. In *New and Future*
1546 *Developments in Microbial Biotechnology and Bioengineering* (pp. 201-208).
1547 Elsevier.

1548 [155] Tiwari, S., & Verma, T. (2019). Cellulose as a Potential Feedstock for Cellulose
1549 Enzyme Production. In *Approaches to Enhance Industrial Production of Fungal*
1550 *Cellulases* (pp. 89-116). Springer, Cham.

1551 [156] Gupta, R., Mehta, G., Deswal, D., Sharma, S., Jain, K. K., Kuhad, R. C., & Singh,
1552 A. (2013). Cellulases and their biotechnological applications. In *Biotechnology for*
1553 *Environmental Management and Resource Recovery* (pp. 89-106). Springer, India.

1554 [157] Menendez, E., Garcia-Fraile, P., & Rivas, R. (2015). Biotechnological applications
1555 of bacterial cellulases. *AIMS Bioengineering*, 2(3), 163-182.

1556 [158] Lupoi, J. S., & Smith, E. A. (2011). Evaluation of nanoparticle-immobilized cellulase
1557 for improved ethanol yield in simultaneous saccharification and fermentation
1558 reactions. *Biotechnology and bioengineering*, 108(12), 2835-2843.

1559 [159] Cho, E. J., Jung, S., Kim, H. J., Lee, Y. G., Nam, K. C., Lee, H. J., & Bae, H. J.
1560 (2012). Co-immobilization of three cellulases on Au-doped magnetic silica
1561 nanoparticles for the degradation of cellulose. *Chemical Communications*, 48(6),
1562 886-888.

1563 [160] Ariaeenejad, S., Motamedi, E., & Salekdeh, G. H. (2020). Stable cellulase
1564 immobilized on graphene oxide@ CMC-g-poly (AMPS-co-AAm) hydrogel for
1565 enhanced enzymatic hydrolysis of lignocellulosic biomass. *Carbohydrate polymers*,
1566 230, 115661.

1567 [161] Huang, W., Pan, S., Li, Y., Yu, L., & Liu, R. (2020). Immobilization and
1568 characterization of cellulase on hydroxy and aldehyde functionalized magnetic
1569 Fe₂O₃/Fe₃O₄ nanocomposites prepared via a novel rapid combustion process.
1570 International Journal of Biological Macromolecules, 162, 845-852.

1571 [162] Xu, J., Sheng, Z., Wang, X., Liu, X., Xia, J., Xiong, P., & He, B. (2016). Enhancement
1572 in ionic liquid tolerance of cellulase immobilized on PEGylated graphene oxide
1573 nanosheets: application in saccharification of lignocellulose. Bioresource
1574 technology, 200, 1060-1064.

1575 [163] Kaur, P., Taggar, M. S., & Kalia, A. (2020). Characterization of magnetic
1576 nanoparticle-immobilized cellulases for enzymatic saccharification of rice straw.
1577 Biomass Conversion and Biorefinery, 1-15.

1578 [164] Utomo, Y., Yuniawati, N., Wonorahardo, S., Santoso, A., Kusumaningrum, I. K., &
1579 Susanti, E. (2019, May). Preliminary study of immobilized cellulase in silica from
1580 the rice husk ash to hydrolysis sugarcane bagasse. In IOP Conference Series: Earth
1581 and Environmental Science (Vol. 276, No. 1, p. 012018). IOP Publishing.

1582 [165] Costantini, A., Venezia, V., Pota, G., Bifulco, A., Califano, V., & Sannino, F. (2020).
1583 Adsorption of Cellulase on Wrinkled Silica Nanoparticles with Enhanced Inter-
1584 Wrinkle Distance. Nanomaterials, 10(9), 1799.

1585
1586
1587
1588
1589
1590
1591
1592
1593
1594
1595
1596
1597

1598 **Figure captions**

1599 **Figure 1** Significant potential of nanomaterials for enzyme immobilization. Reprinted from
1600 Ref. [17] with permission from Elsevier. License Number: 5081540394562.

1601 **Figure 2** Advantages of nanomaterials as enzyme immobilization platforms.

1602 **Figure 3** Stepwise illustration of cellulose-deconstruction potential of cellulase based
1603 nano-biocatalytic systems as a strategic drive from designing to sustainable applications.

1604 **Figure 4** Schematic illustration of the preparatory method of chitosan/magnetic porous
1605 biochar as support for cellulase immobilization in the presence of glutaraldehyde (GA) as
1606 a cross-linker. Initially, sugarcane bagasse was used to prepare biochar via pyrolysis in
1607 the presence of potassium hydroxide (KOH). In the following step, calcination was
1608 performed to engineer magnetic biochar which was subjected to chitosan coating and
1609 used for cellulase immobilization by GA activation. The bar graph given in red color at the
1610 bottom left corner shows the effect of recycling on the glucose productivity of immobilized
1611 cellulase. Reprinted from Ref. [53] with permission under the terms and conditions of the
1612 Creative Commons Attribution (CC BY) license.

1613 **Figure 5** The process of construction of bioconjugates. Reprinted from Ref. [58] with
1614 permission from Elsevier. License Number: 5081660389521.

1615 **Figure 6** Cellulase immobilization on iron oxide nanoparticle surfaces. Reprinted from
1616 Ref. [78] with permission from Springer Nature. License Number: 5081660693327.

1617 **Figure 7** Potential advantages of CLEAs. Reprinted from Ref. [86] with permission from
1618 Taylor & Francis. License Number: 5081660850455.

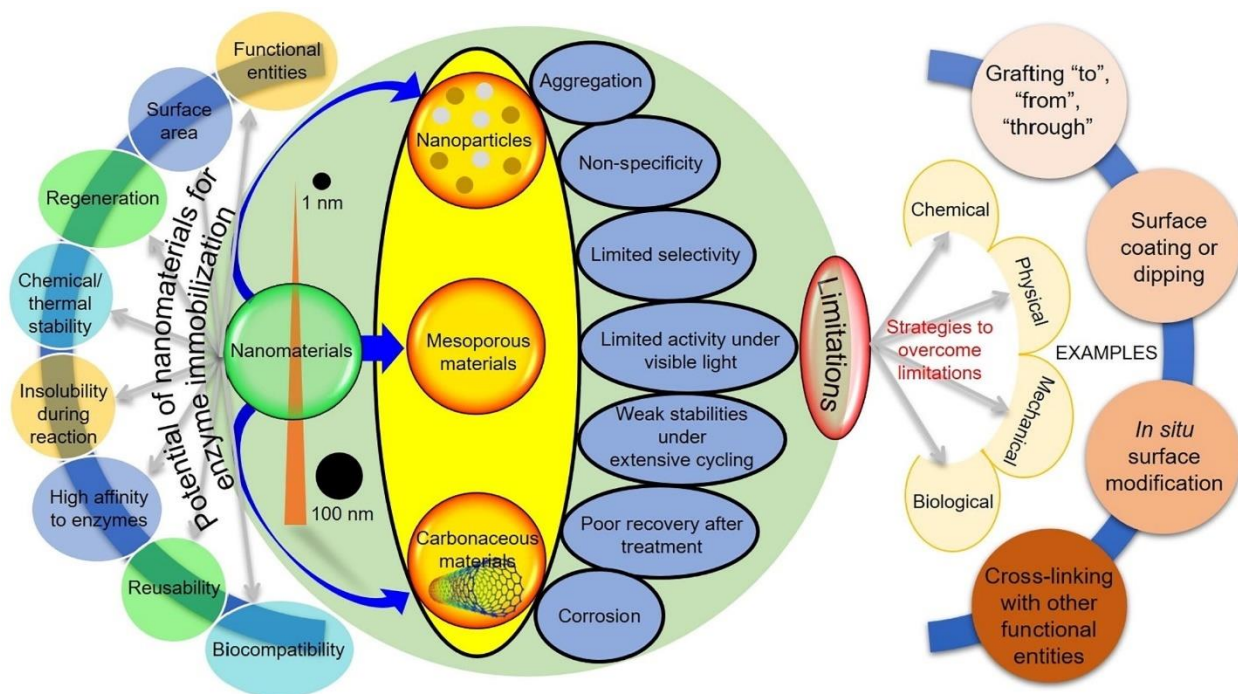
1619 **Figure 8** Diagrammatic sketches of enzyme immobilization onto MOF surface by covalent
1620 grafting. (A) Direct covalent grafting between MOF and enzyme; (B) A dye-tagging
1621 strategy for enzyme immobilization on MOF surface. Reprinted from Ref. [130] with
1622 permission from Elsevier. License Number: 5081660986472.

1623 **Figure 9** Bioconversion of lignocellulosic biomass to fermentable sugars by immobilized
1624 magnetic cellulolytic enzyme cocktails. Reprinted from Ref. [135] with permission from
1625 American Chemical Society.

1626 **Figure 10** Approaches to enhance biofuels production in the presence of cellulase.
1627 Reprinted from Ref. [6] with permission from Elsevier. License Number: 5081661163485.

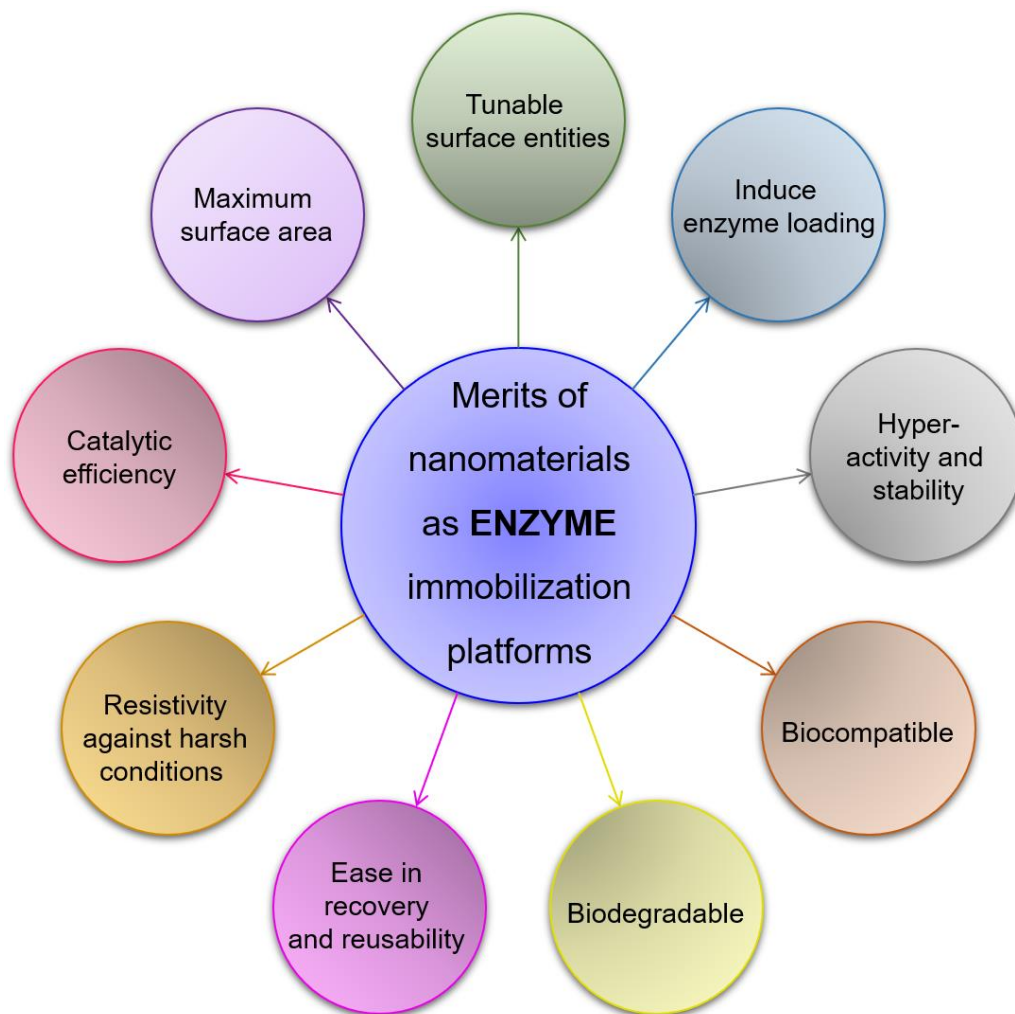
1628

1629 **List of Figures**



1630
1631 **Figure 1**

1632
1633
1634
1635
1636
1637
1638
1639
1640
1641
1642
1643
1644
1645
1646
1647



1648
1649
1650
1651
1652
1653
1654
1655
1656
1657
1658
1659
1660

Figure 2

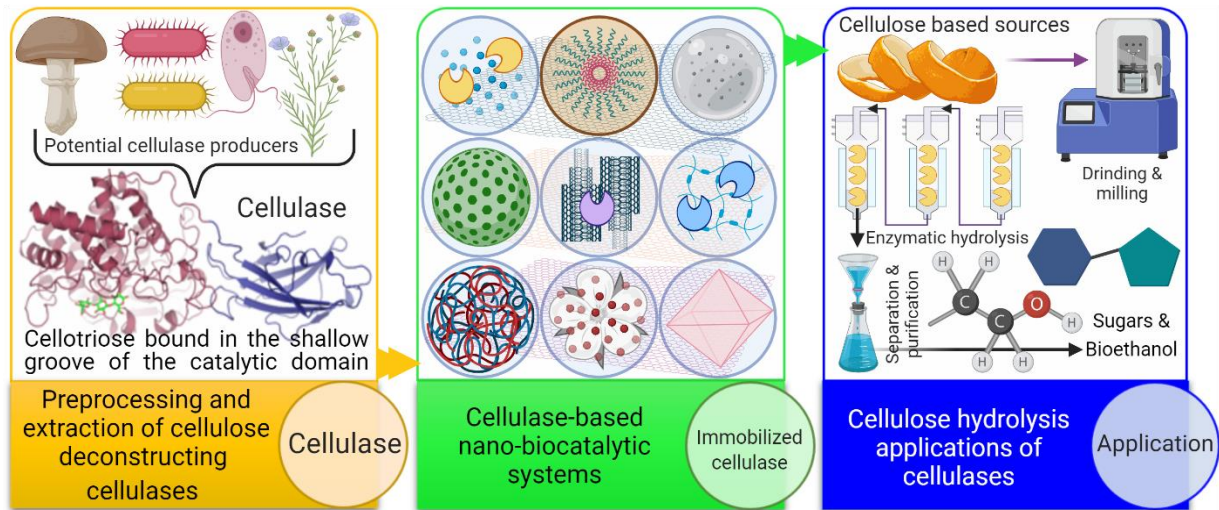
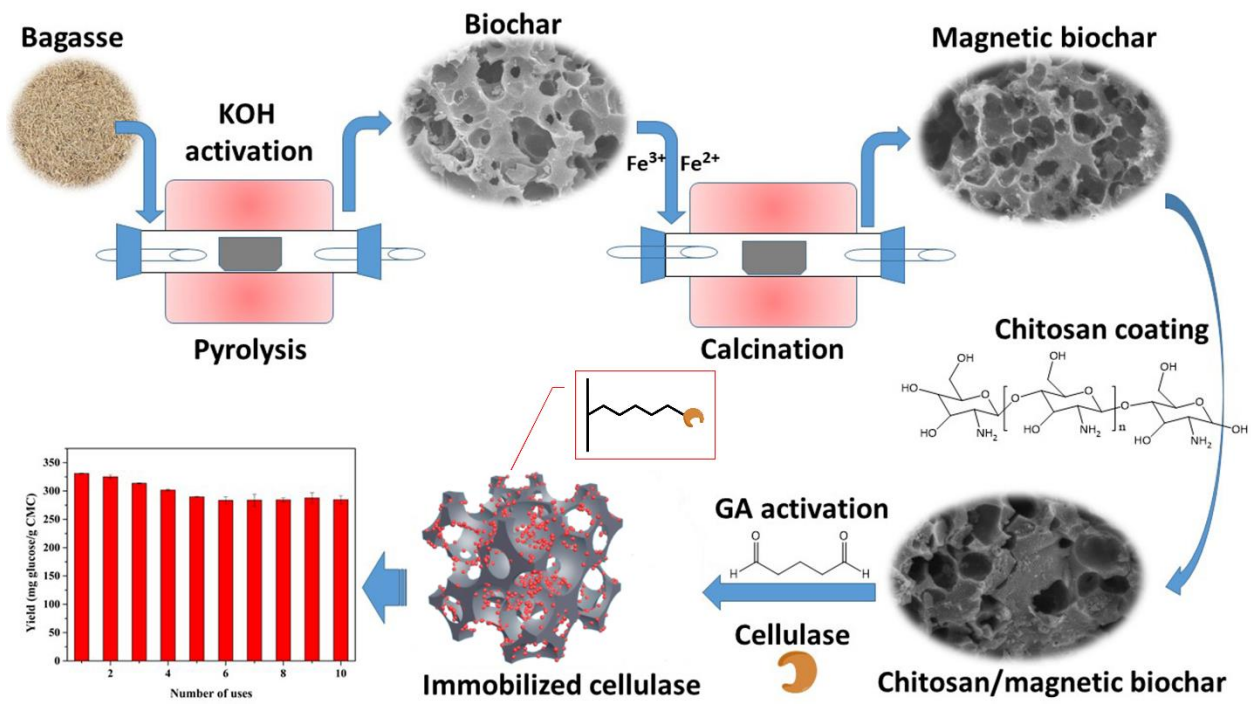


Figure 3

1661
 1662
 1663
 1664
 1665
 1666
 1667
 1668
 1669
 1670
 1671
 1672
 1673
 1674
 1675
 1676
 1677
 1678
 1679
 1680
 1681
 1682



1683

1684

Figure 4

1685

1686

1687

1688

1689

1690

1691

1692

1693

1694

1695

1696

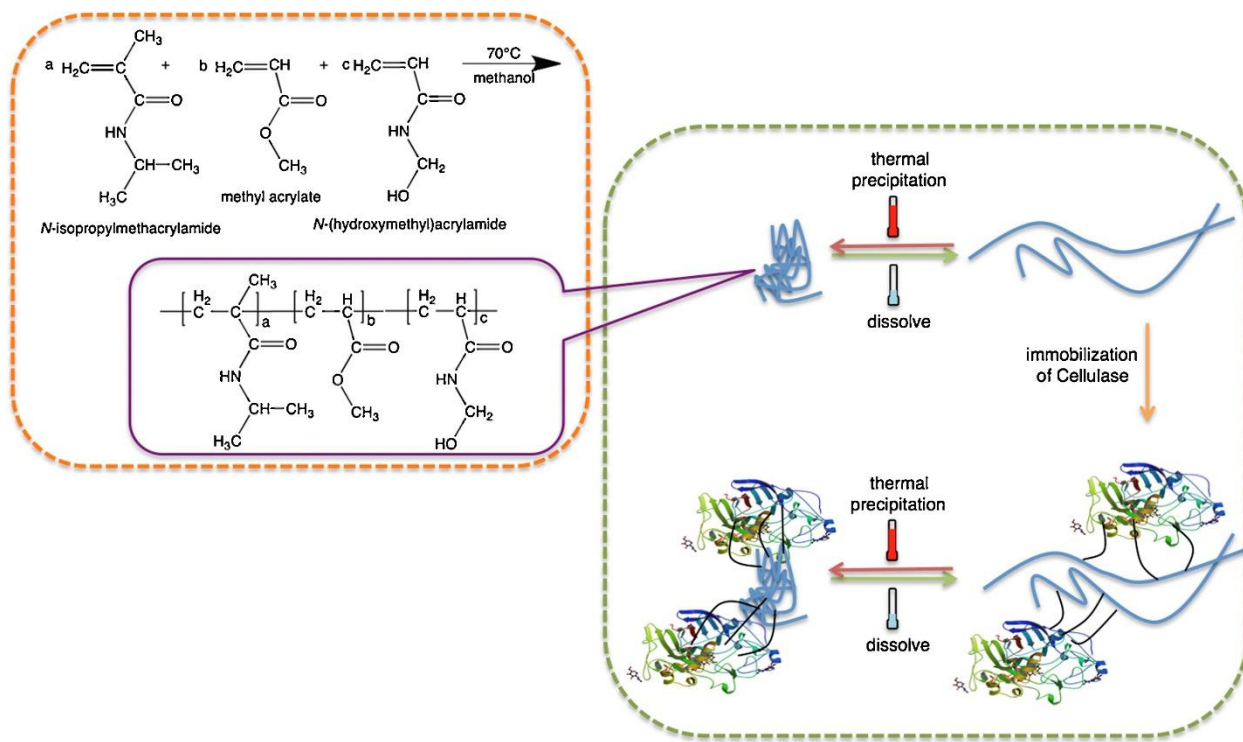
1697

1698

1699

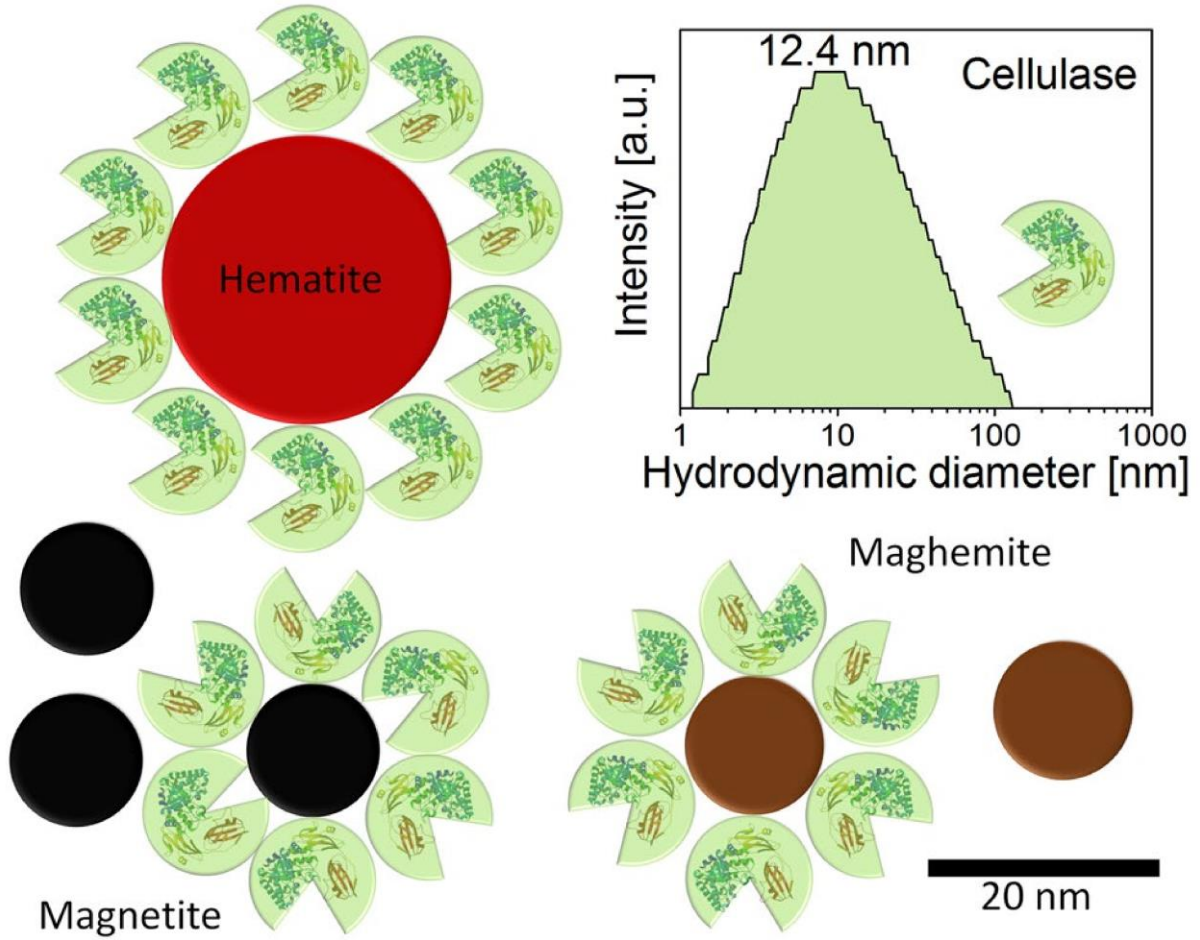
1700

1701



1702
 1703
 1704
 1705
 1706
 1707
 1708
 1709
 1710
 1711
 1712
 1713
 1714
 1715
 1716
 1717
 1718
 1719
 1720

Figure 5



1721

1722 **Figure 6**

1723

1724

1725

1726

1727

1728

1729

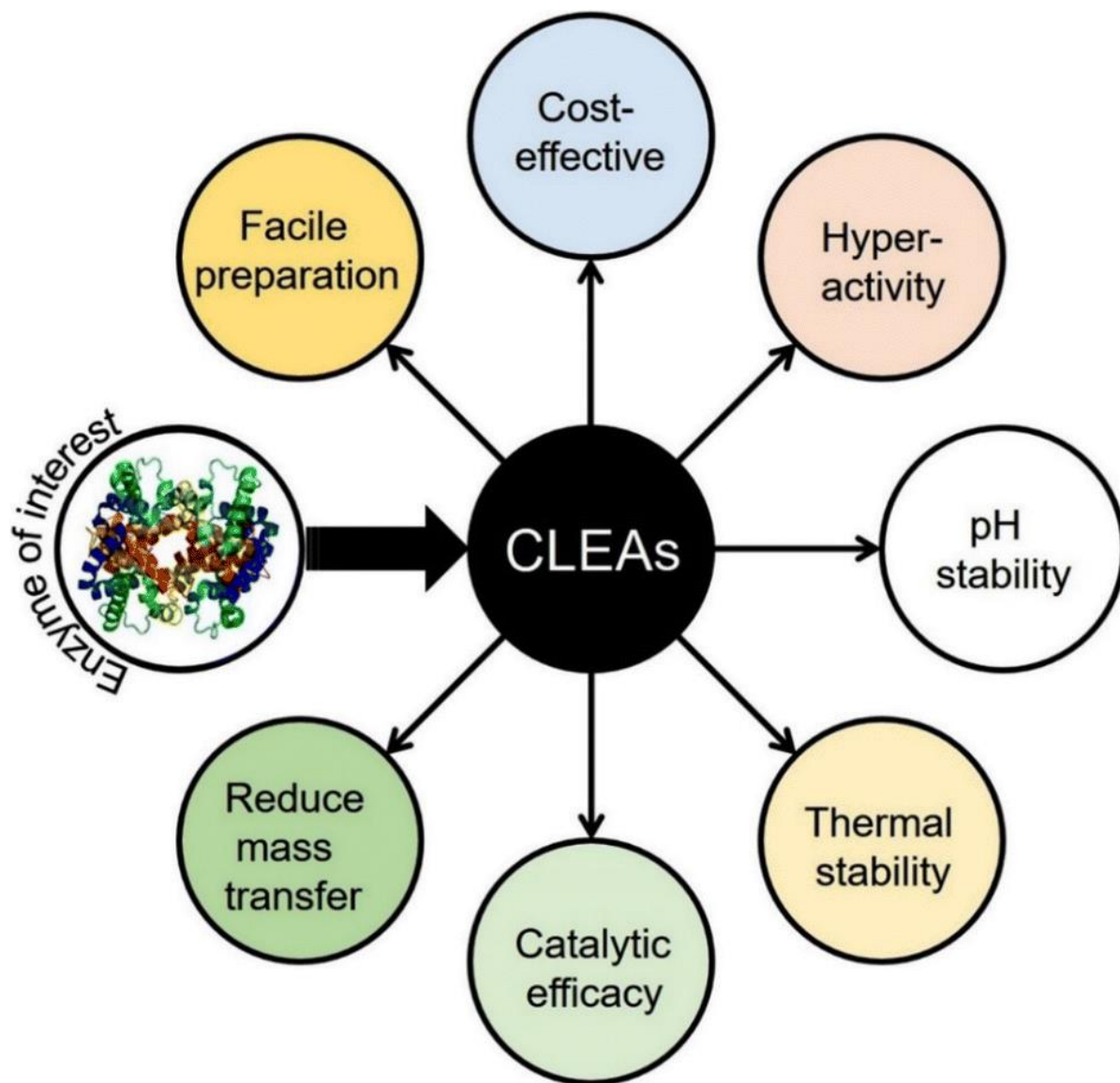
1730

1731

1732

1733

1734



1735

1736 **Figure 7**

1737

1738

1739

1740

1741

1742

1743

1744

1745

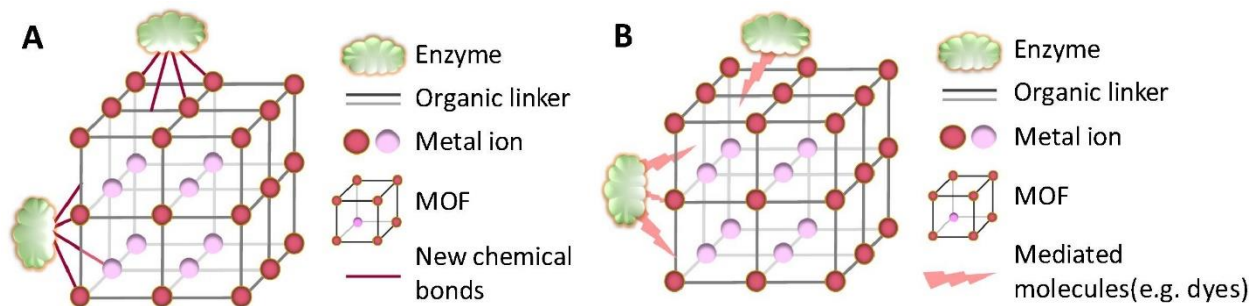
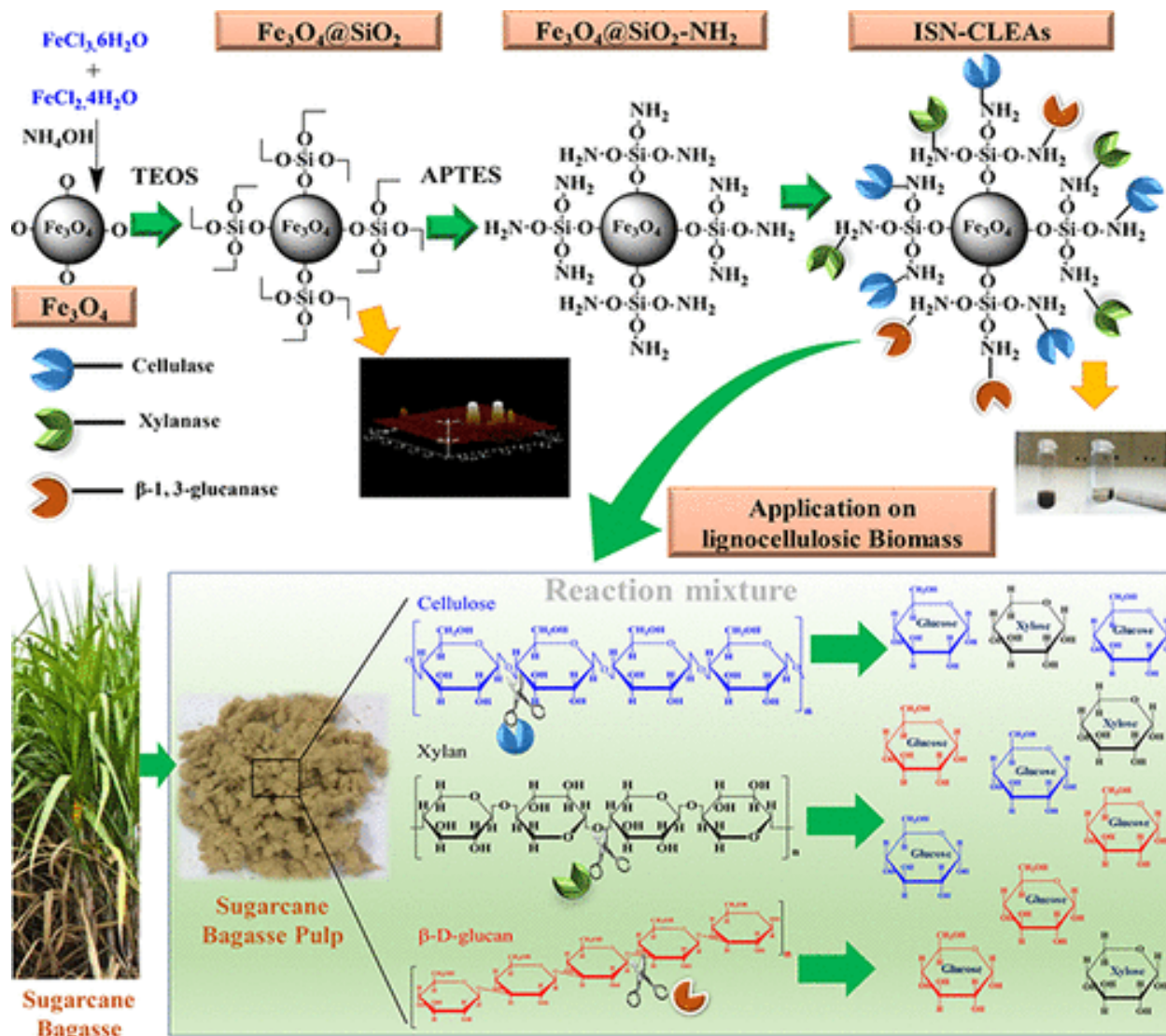


Figure 8

1746
 1747
 1748
 1749
 1750
 1751
 1752
 1753
 1754
 1755
 1756
 1757
 1758
 1759
 1760
 1761
 1762
 1763
 1764
 1765
 1766
 1767
 1768
 1769
 1770
 1771



1772

1773

Figure 9

1774

1775

1776

1777

1778

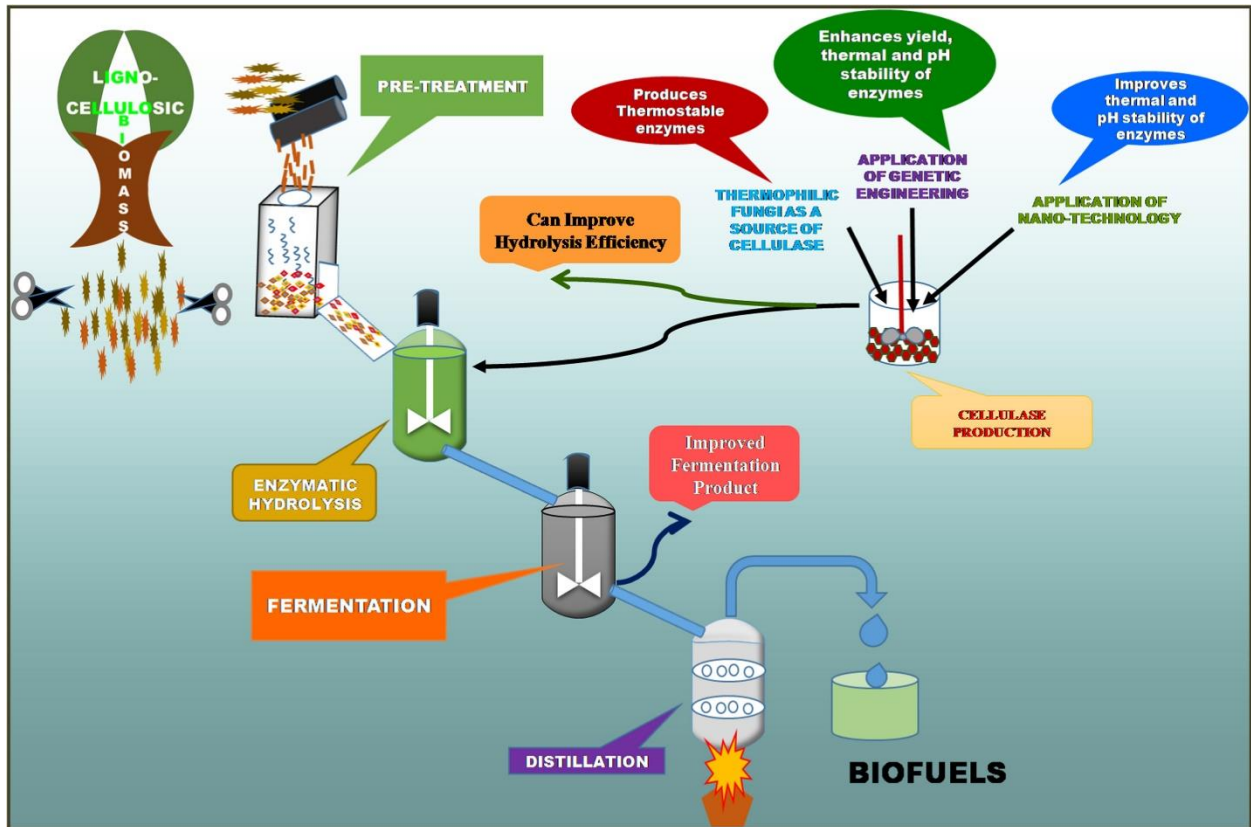
1779

1780

1781

1782

1783



1784

1785 **Figure 10**

1786

1787

1788

1789

1790

1791

1792

1793

1794

1795

1796

1797

1798

1799

1800

1801 **List of Tables**

1802 **Table 1** Polymer-based supports for cellulase immobilization with binding method,
 1803 stability/recyclability, and industrial applications.

Immobilization support	Binding method	Stability/ Recyclability potential	Industrial applications	References
Ca-alginate	Entrapment	High activity retention up to four cycles	-	[41]
Ca-alginate-xerogel matrix	Entrapment	-	Fruit juice clarification	[42]
Na-alginate polyethylene	Glutaraldehyde crosslinking	Up to 53% activity after 3 cycles	Enzymatic MCC hydrolysis	[43]
Ca-alginate	Entrapment	45% retention after 3 days, with stability at 4 °C for 12 days and at 30 °C for 3 days	Enzymatic CMC hydrolysis	[41]
Ca-alginate	Entrapment	69.2% activity retention after 5 cycles	-	[44]
Chitosan-Magnetic NPs	Entrapment	Excellent thermal stability at 80 °C	-	[46]
Chitosan amino condensation adduct	Crosslinking and covalent attachment	Up to 70% activity retention after 25 cycles	-	[49]
Chitosan-iron oxide	Glutaraldehyde crosslinking	No significant loss for 3 consecutive cycles	-	[50]
Chitosan-magnetic nanoparticles	Chemical crosslinking	Up to 80% activity retention for 15 cycles	Lignocellulose hydrolysis	[28]
Chitosan-magnetic nanoparticles	Alkaline precipitation	High stability	-	[51]
Chitosan-porous biochar	Covalent linking	-	Enzymatic CMC hydrolysis	[53]

1804

1805 **Table 2** Nanocarriers for cellulase immobilization with binding method,
 1806 stability/recyclability, and industrial applications.

Immobilization support	Binding method	Stability/ Recyclability potential	Industrial applications	References
MWCNT	Covalent binding	-	Fruit bunches degradation	[115]
GO@CMC- <i>g</i> -poly(AMPS-co-AAm)	Physical crosslinking	90.5% activity retention after 5 cycles	Lignocellulosic biomass hydrolysis	[160]
MWCNT	Physical absorption	52% activity retention after 6 cycles	Food and agricultural sector applications	[113]
Functionalized Fe ₂ O ₃ /Fe ₃ O ₄ nanoparticles	Novel rapid combustion method	71% activity retention after 5 cycles	-	[161]
PEGylated GO nanosheets	Chemical linking	Up to 73% activity retention after 3 cycles	Saccharification of lignocellulose	[162]
Magnetic iron oxide nanoparticles	Glutaraldehyde crosslinking	50.34% activity retention after 4 saccharification cycles	Saccharification of rice straw	[163]
Rice husk silica ash	Physical adsorption	58.8% activity retention after 3 cycles	Hydrolysis of sugarcane bagasse	[164]
Core-shell mesoporous magnetic AuNPs	Chemical method	57% activity retention after 4 cycles	-	[63]
Wrinkled silica nanoparticles	Physical adsorption	High recyclability	-	[165]
Mesoporous silica (SBA-15)	Encapsulation	Up to 70% activity retention after four weeks incubation	-	[66]
Mesoporous silica (FDU-12)	Physical adsorption	Almost 100% of its activity retention after 15 days incubation	-	[67]
Iron oxide nanoparticles	Physical adsorption	High recyclability	-	[78]

1807